Taylor & Francis
Taylor & Francis Group

European Journal of Environmental and Civil Engineering

ISSN: (Print) (Online) Journal homepage: https://www.tandfonline.com/loi/tece20

Combined effect of using steel fibers and demolition waste aggregates on the performance of fly ash/slag based geopolymer concrete

Asfaw Mekonnen Lakew, Orhan Canpolat, Mukhallad M. Al-Mashhadani, Mucteba Uysal, Anıl Niş, Yurdakul Aygörmez & Mohammad Bayati

To cite this article: Asfaw Mekonnen Lakew, Orhan Canpolat, Mukhallad M. Al-Mashhadani, Mucteba Uysal, Anıl Niş, Yurdakul Aygörmez & Mohammad Bayati (2023): Combined effect of using steel fibers and demolition waste aggregates on the performance of fly ash/slag based geopolymer concrete, European Journal of Environmental and Civil Engineering, DOI: 10.1080/19648189.2023.2189468

To link to this article: https://doi.org/10.1080/19648189.2023.2189468

Published online: 13 Mar 2023.

EUROPEAN JOURNAL OF ENVIRONMENTAL AND CIVIL ENGINEERING
https://doi.org/10.1080/19648189.2023.2189468

Taylor & Francis
Taylor & Francis Group

Check for updates

Combined effect of using steel fibers and demolition waste aggregates on the performance of fly ash/slag based geopolymer concrete

Asfaw Mekonnen Lakew[a], Orhan Canpolat[a], Mukhallad M. Al-Mashhadani[b], Mucteba Uysal[a], Anıl Niş[b], Yurdakul Aygörmez[a] and Mohammad Bayati[a]

[a]Faculty of Civil Engineering, Civil Engineering Department, Yildiz Technical University, Istanbul, Türkiye; [b]Faculty of Architecture and Engineering, Civil Engineering Department, Istanbul Gelisim University, Istanbul, Türkiye

ABSTRACT

Developing sustainable construction products has been showing a rising trend recently. Geopolymer composites are remarkable binding materials fabricated based on recycling and sustainability. In this paper, an experimental investigation was conducted to study some mechanical and durability characteristics of steel fiber-reinforced fly ash/slag-based geopolymer concrete (GPC) with different proportions of recycled coarse aggregate. Steel fiber-reinforced geopolymer concrete mixtures incorporating recycled coarse aggregates of up to 40% at the interval of 10% were prepared, and the mixtures without recycled coarse aggregate were used as reference samples. The steel fiber ratio of 0.3% and 0.6% were used and the combined effect of steel fiber and recycled coarse aggregate on the geopolymer composites' behavior regarding strength properties, sulfate resistance, elevated temperature resistance, abrasion resistance, and freezing-thawing resistance was addressed. A significant improvement in strength properties was observed in steel fiber reinforced recycled aggregate geopolymer concrete with increasing fiber content; however, the strength properties of geopolymer concrete were decreased with the increase of recycled coarse aggregate amount. Also, the properties such as abrasion resistance, resistance to elevated temperature, sulfate resistance, and freeze-thaw resistance were improved with the addition of steel fiber. It indicates that the synergetic effect of steel fiber and recycled aggregate helps to produce ecologically sound geopolymer concrete with good engineering properties and durability characteristics that will bring sustainability to the concrete sector. Generally, the results show that the recycled coarse aggregate ratio of up to 30% and 0.6% of steel fiber can be considered an ideal combination to make geopolymer concrete with better overall properties.

ARTICLE HISTORY
Received 17 May 2022
Accepted 13 January 2023

KEYWORDS
Geopolymer; fly ash; slag; recycled coarse aggregate; steel fibers; strength properties; durability properties

1. Introduction

The concrete industry, believed to be the driving force of modern construction, has numerous drawbacks regarding environmental issues and sustainability. Conventional construction technologies release a large amount of Greenhouse Gas (GHG) into the atmosphere due to its crucial ingredients, such as clinker. According to the studies, a tone of Portland cement production loads approximately one-tonne Carbon

CONTACT Mukhallad M. Al-Mashhadani mashhadani@gelisim.edu.tr Faculty of Architecture and Engineering, Civil Engineering Department, Istanbul Gelisim University, Avcilar Campus, Istanbul, Türkiye.

dioxide (CO_2) into the environment (Malhotra, 2002). Furthermore, one ton of ordinary Portland cement manufacturing consumes approximately 1.7 tons of raw materials.

Due to the profound impact of ordinary Portland cement (OPC) on the natural ecosystem, several studies have addressed various possible measurements, mainly focusing on reducing emissions of clinker production and limiting the content of clinker hired through new technologies (Taylor et al., 2006). The utilization of high-volume cementitious elements as the partial replacement of Ordinary Portland Cement (OPC) was also considered a possible alternative to overcome the listed limitations of conventional cement (Ebrahimi et al., 2017). Recently, hiring completely non-cement binders known as geopolymers is gaining momentum (Schneider et al., 2011), which is thought to be an excellent shift to reduce world clinker production. Studies demonstrated that employing geopolymer products in the concrete industry may reduce global CO_2 emissions by an average of 85% (Davidovits, 1994).

Geopolymer, becoming a primary focus of recent green technology, is a product of base materials owing to the high alumina and silica content. The precursor elements are from industrial waste, fly ash, slag, or geologic products such as metakaolin. Geopolymers usually obtain strength through the geopolymerization process. Fly ash-slag-based geopolymer exhibits a complex reaction that encompasses the hydration of calcium oxide (Kumar et al., 2010; Ye & Radlińska, 2016), giving a calcium silicate hydrate modified with aluminum (CASH) as a primary binding phase. In the geo-polymerization process, alkalization of the alumina and silica-enriched elements entails the dissolution of silica and alumina followed by coagulation and then a highly exothermic condensation reaction followed by crystallization leading to the creation of a three-dimensional network of the amorphous alumina-silicate hydrate binder (Ismail et al., 2014; Ye & Radlińska, 2016), which possess different reaction mechanism from that of OPC

Also, geopolymers have various benefits in maintaining a binder owing to a low embodied energy and less CO_2 release (Provis et al., 2015). Fly ash/slag-based GPC hardens at room temperature. Furthermore, most geopolymer products are not hostile to handle and store. Moreover, geopolymer concrete does not need a particular mixing procedure; therefore, it can be quickly hired for a potential replacement of OPC Geopolymer-based concrete possesses outstanding mechanical and durability characteristics. It was demonstrated in studies (Davidovits, 1991; Provis et al., 2015).

Ahmet et al. (Kurtoglu et al., 2018) indicated that slag-based GPC specimens cured at room temperature undergo higher compressive and tensile strength than concrete produced from ordinary Portland cement and fly ash only. Hardjito et al. (Hardjito et al., 2004) Obtained significantly higher compressive performance for low calcium fly ash-based geopolymer concrete cured at elevated temperatures. Therefore, it is possible to attain higher compressive strength and low calcium geopolymer products by introducing heat activation that facilitates the geo-polymerization process. Ahmet et al. (Kurtoglu et al., 2018) studied the impact of chemical aggression on the durability characteristics of GPC and OPC concrete. They used visual inspection and weight loss measurements to determine the effect of an acidic, sulfate, and marine environment on test specimens. According to their study, conventional concrete experienced the most significant surface deterioration; slag and fly ash-based geopolymers experienced moderate and slight surface deterioration after exposure to chemical attacks. Sulfuric acid aggression is perceived to be the most severe attack. Also, the rate of mechanical performance decline in OPC concrete has been slightly higher than the drop in the case of the geopolymer concrete matrix. Chen Huiguo et al. (Junru et al., 2019) investigated the response of fly ash/slag-based geopolymer concrete exposed to various degrees of high temperature. According to the study, GPC specimens have shown fewer surface changes such as color change, mass loss, cracks, and corner breakage than conventional cement concrete specimens. Some strength parameters of OPC concrete samples exposed to elevated temperature have significantly declined compared to specimens at room temperature. In contrast, GPC specimens subjected to high temperature possessed the greatest compressive strength at 400 °C; however, it showed considerable reduction after 400 °C. In the study by Kumar et al. (Kumar et al., 2010), a fly ash/slag-based geopolymer matrix is anticipated to result in better thermal characteristics than its OPC encounter.

These days, construction, and demolition waste (CDW) are significantly increasing worldwide. For instance, in the European Union countries, the annual CDW is estimated to be over 450 million tons, of which only 25% is recycled (E.C. \(European Commission\), Directorate-General Environment, Directorate Industry and Environment, 2000). China's value turns to more than 1.5 billion tons, according to a study taken in 2016 (Sun et al., 2015). However, the utilization rate holds only 10% of the total production. CDW are foes to the natural ecosystem if they cannot be appropriately managed because conventional disposal of these wastes requires storage and contributes to carbon emissions, heading to critical environmental problems (Colangelo & Cioffi, 2017).

Furthermore, the deterioration of raw materials is abruptly increasing, which prospects the inclusion of RCA in the synthesis of concrete to be a promising alternative for both utilization of CDW and the conservation of environmental and natural resources. Moreover, one of the best solutions to mitigate the drawbacks of the CDW is re-employing Construction and demolition wastes as a recycled construction input like recycled aggregates (Kurda et al., 2018). Ping and Yidong (Ping & Yidong, 2011) indicated that the concrete produced from recycled aggregate is an ideal eco-material. Marie and Quiasrawi (Marie & Quiasrawi, 2012) indicated that up to 20% of substituting virgin aggregate with recycled concrete helped the manufacturing of good quality concrete without harming natural resources and the environment.

Several researchers have addressed the effect of utilizing recycled aggregates instead of natural aggregates to produce geopolymer concrete. Nuaklong et al. (Nuaklong et al., 2016) presented that geopolymer concrete with recycled aggregate resulted in lower compressive strength than conventional concrete with raw aggregate. Nevertheless, the flexural and splitting tensile strength of the recycled aggregate geopolymer concrete was slightly higher than the standard aggregate concrete provided that sodium hydroxide concentration was fixed to 12 M. The density and abrasion resistance of recycled aggregate geopolymer concrete appeared lower than that of natural aggregate geopolymer concrete. In the study by Naga et al. (Sai, 2018), the strength properties of geopolymer concrete with a recycled aggregate ratio of up to 40% experienced a minimum reduction with the addition of recycled aggregate. The decrement rate after 40% replacement was adverse, which might limit the concrete's usability for structural applications. Mesgari et al. (Mesgari et al., 2020) demonstrated that the 50% and 100% replacement ratio of recycled coarse aggregate has resulted in a significant strength reduction in the case of both conventional and geopolymer concrete matrix, although geopolymer concrete appeared more resilient in comparison with OPC concrete.

Hwang et al. (Hwang et al., 2013) revealed that recycled aggregate concrete exhibits lower durability characteristics such as chloride resistance, sulfate attack, and frost action than reference natural aggregate specimens. Ammar and Jasem (Ben Nakhi & Alhumoud, 2019) found that the chloride invasion increased with an increased recycled aggregate replacement level after 28 days of exposure to marine water with a 3% chloride concentration. However, after 14 days of saturation, concrete specimens with a 30% recycled aggregates replacement ratio revealed the lowest chloride diffusion than plain OPC concrete. Geopolymer concrete showed better durability performance than ordinary Portland cement in a sulfuric acid solution, which was revealed by Ariffin et al. (Bhutta et al., 2013). Moreover, Liu et al. (Liu et al., 2016) carried out the microstructural characterization of the new interfacial transition zone in geopolymer concrete blends with re-used aggregates and observed that feeble transitional interphase does not create. Topal et al. (Topal et al., 2022) analyzed the effects of elevated temperatures on the properties of geopolymer concretes containing recycled concrete aggregate and found that the compressive strengths of the samples decreased with increasing RCA ratio in the mixture.

The idea of enhancing the properties of building materials with fiber is an ancient trend (Naaman, 1985). Fibers in concrete that are randomly arranged mitigate the micro-cracking process that causes cracks and restricts crack spread, thus enhancing strength and reducing concrete brittleness (Bencardino et al., 2008). Including fibers in concrete improves elastic modulus, increases ductility, and makes concrete more homogeneous and isotropic (Bencardino et al., 2008; Faisal & Ashour, 1992). Bentur et al. (Bentur & Mindess, 1990) mentioned factors that affect the properties of fiber-reinforced concrete. These include the fiber type, size, length-to-width ratio, and volume fraction of the fiber used.

Osama et al. (Zaid et al., 2022) studied the performance of metakaolin-based steel fiber-reinforced geopolymer concrete produced with the partial replacement of natural coarse aggregate with recycled one. The study revealed that the incorporation of steel fiber caused an insignificant change in the compressive performance of the concrete matrix. However, other properties such as drying shrinkage, flexural, and splitting tensile strength saw a significant change with the addition of steel fiber. The authors concluded that a mix containing 25% RCA and 3% steel fiber could be an ideal proportion to maintain both the environmental and strength aspect of the composite matrix.

Raphaela et al. (Gomes et al., 2020) analyzed the fracture parameters of steel fiber-reinforced geopolymer concrete. The study revealed the significance of steel fiber in reducing crack distribution and curbing the brittle nature of the resulting composites. According to this investigation, all the fracture parameters improved by including fibers. The concrete specimens produced by incorporating 0.5% steel reinforcement gave the most significant improvement compared to the unreinforced ones.

The mechanical characteristics of fly ash-based geopolymer reinforced with steel micro-fibers were investigated by Ranjbar et al. (Ranjbar et al., 2016). The study indicated that the resulting composite's bending strength and energy absorption capacity was enhanced with the addition of steel microfibers. Kuranli et al. (Kuranlı et al., 2023) studied the properties of steel, polypropylene, and polyamide fiber-reinforced slag-based alkali-activated concrete and reported that adding fibers significantly improved the strength and durability properties of samples. Nis et al. (Niş et al., 2023) used recycled tire rubber and steel fiber in slag-based self-compacting alkali-activated concrete. They reported that the incorporation of fine and coarse crumb rubbers reduced the mechanical properties, and the reduction was found more with increased rubber contents, whereas the incorporation of steel fiber compensated for the strength loss.

Xiaolu and Xuejiao (Guo & Pan, 2018) analyzed the impact of polypropylene, basalt, and steel fiber on geopolymer composites' microstructural and mechanical properties. The report indicated that the late-age mechanical performance of the fly ash and slag-based geopolymer matrix was improved with the addition of polypropylene and basalt fiber additives. At the same time, the toughness and reinforcement impact was significantly enhanced when steel fiber was used. Also, limited crack propagation and lower pore development were demonstrated due to the inclusion of fibers. Steel fiber has recorded an outstanding performance compared to polypropylene and basalt fibers. According to the study by Sukontasukkul et al. (Sukontasukkul et al., 2018), the synergetic effect of the fibers has shown better performance in terms of toughness, flexural, and residual strengths than sole polypropylene addition. The toughness and residual strength appeared proportional to the steel fiber content. The impact of polypropylene fibers on the metakaolin-based geopolymer concrete produced, with the partial replacement of recycled aggregates, was evaluated by Behforouz et al. (Behforouz et al., 2020). The polypropylene fibers appeared worthwhile in flexural strength, split tensile strength, and geopolymer matrix drying shrinkage.

Moreover, the load-deflection curve improvement was observed with the polypropylene fiber ratio increase. It, in turn, resulted in higher fracture toughness and better maximum load potential. Furthermore, the microstructural assessment showed that the polypropylene fiber significantly restricts possible crack distribution due to the bonding between fibers and the geopolymer binder.

Several scholars demonstrated that recycled aggregate gives an excellent alternative aggregate for producing concrete in terms of environmental acceptability and economic feasibility (Marinković et al., 2010; Ping & Yidong, 2011). It is also reported that recycled aggregate may negatively impact the concrete matrix's mechanical and durability properties. In this study, recycled aggregate is used in combination with steel fiber. Steel fibers are the most widely employed type of fiber in concrete production. They help enhance concrete ductility, toughness, and the ability to withstand crack development (Xie et al., 2015). However, the impact of steel fiber on the mechanical properties of the resulting matrix directly depends on its content (Xie et al., 2015). It is also revealed that fibers can mitigate crack development and minimize micro-crack distribution in the geopolymer concrete, hence improving the resulting matrix's mechanical and durability properties. As a result, investigating the synergetic effect of recycled coarse aggregate and steel fiber will help to develop eco-friendly construction material while maintaining appropriate engineering properties.

Furthermore, this study used ten different materials, such as fly ash and slag as the main binder of the geopolymer, recycled aggregate, and natural aggregate to substitute coarse aggregates, river sand and crushed limestone sand as fine aggregates, a combination of NaOH and sodium silicate as alkaline activators, steel fibers and superplasticizer for admixtures. No detailed investigation is conducted on the synergetic effect of steel fibers and recycled coarse aggregate on this type of complex geopolymer concrete matrix, which confirms the novelty of this paper. This experimental work aims to fill the vacuum to produce environment-friendly concrete with better engineering properties by utilizing construction and demolition wastes (RCA) and steel fibers. This study demonstrates the appropriateness of recycled coarse aggregate and steel fiber in fly ash/slag-based geopolymer concrete. The study evaluated the mechanical and durability properties of fly ash-based geopolymer concrete through compressive strength, splitting tensile strength, flexural strength, abrasion resistance, high-temperature resistance, sulfate attack resistance, and freeze-thaw resistance. Moreover, scanning electron microscopy (SEM) and Fourier Transform Infrared Spectroscopy (FTIR) analysis were done to understand the microstructural characteristics of the matrix. This paper contributes to the efforts towards creating a sustainable construction industry through re-employing construction and demolition wastes as aggregates and producing cement-free concrete.

2. Materials characterization

2.1. Materials

Low calcium fly ash (Class F) confirming the standard specifications stipulated in ASTM C618 (ASTM C618-19,19, 2019) was obtained from Cateş Elektrik Üretim A.Ş. Çatalağzı/Zonguldak, a thermal power plant based in Turkey. Bolu Çimento Company provided Ground Granulated Blast Furnace Slag (GGBS). The chemical composition of fly ash and slag is given in Table 1. A mixture of NaOH and Na_2SiO_3 solution was chosen as a chemical activator to produce slag/fly ash-based fiber-reinforced geopolymer concrete. A carboxylic ether polymer with long side chains in liquid form, under the brand name Master Glenium 51, supplied by BASF Türk Kimya San. ve Tic. Ltd. company, based in Türkiye, was used to enhance the workability of the fresh concrete without using excess water. The product specifications appear in Table 2. Also, crimpled steel fibers obtained from the local supplier named KrampeHarex İnşaat Mühendislik Yapı Ürünleri Sanayi ve Ticaret Ltd. was used. The technical specifications of the fibers are given in Table 3.

In this investigation, natural river sand and crushed sand having a specific gravity of 2.7 and 2.65, respectively, were used as fine aggregates. An equal proportion of Natural River and crushed limestone sand were contributed to make up a fine aggregate with Dmax 4 mm.

Recycled and natural coarse aggregates were supplied from local sources. Coarse aggregates of 12–22mm and 4–12mm were identified as NO. II and NO. I, respectively. The recycled coarse aggregate was obtained from demolished buildings near Istanbul. The specific gravity and water absorption capacity of natural coarse aggregates were evaluated as 2.71 and 1.2%, respectively. These values for recycled coarse aggregates were recorded at 2.57 and 6.8%, respectively. It can be seen that recycled coarse aggregate exhibits high water absorption capacity. The attached mortar and the rough surface of the recycled coarse aggregates are the possible reasons for the higher water absorption capacity of the recycled aggregates. No preparation was made on the recycled coarse aggregates during mixing except pre-wetting based on their water absorption capacity. The particle size distribution of RCA is given in Figure 1.

3. Experimental procedure

3.1. Mix design and mixing

Concrete specimens were manufactured according to the standard mixing procedure mentioned in Figure 2. Series of concrete mixtures with the addition of recycled coarse aggregates of up to 40% at the interval of 10% were produced and compared with the reference mixture manufactured without recycled coarse aggregate.

Table 1. Chemical composition of fly ash and slag.

	Content (%)	
Oxides	Fly ash	Slag
SiO_2	58.75	40.55
Al_2O_3	25.24	12.83
Fe_2O_3	5.76	1.1
CaO	1.46	35.58
MgO	2.22	5.87
SO_3	0.008	0.18
Na_2O	0.60	0.79
Free CaO	0.11	–
Cl^-	0.015	0.014
K_2O	4.05	–
LOI	1.12	0.03
TiO_2	–	0.75

Table 2. Characteristics of the superplasticizer used.

Chemical Description	Modified Polycarboxylic Ether Based
Name	Master Glenium 51
Color	Dark brown
State	Liquid
PH Value	6-7
Specific gravity (kg/l) @ 20°C	1.082 – 1.142
Chloride content (%)	=< 0.1 (by mass)
Alkali content (%)	=< 3 (by mass)
Recommended dosage	1-2% (% binder content)

Table 3. Properties of crimpled steel fiber utilized in the study.

Characteristics	Value
Fiber type	Crimpled steel
Width (d) (mm)	2.30 / 2.95
Length (l) (mm)	50 ± 10%
Cross-section	Straight
Tensile Strength (MPa)	800 ± 15%

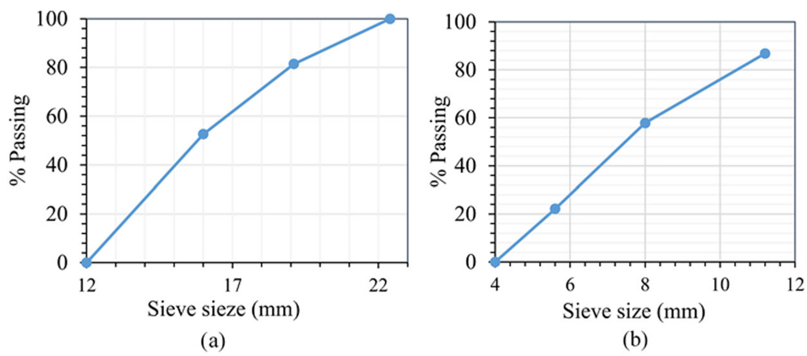

Figure 1. (a) Gradation of NO. II recycled coarse aggregate (b) Gradation of NO. I recycled coarse aggregate used.

In addition, steel fibers were incorporated as a volume fraction ratio of 0.3% and 0.6% for every series of mix designs iteratively. Recycled coarse aggregate proportion and steel fiber ratio were chosen based on the trial mix results and in agreement with past research to determine the combined effect of recycled coarse aggregate and steel fibers on the various properties of geopolymer concrete. Chemical solutions to binder ratio of 0.5 were adjusted by trial and error by considering appropriate compressive strength and workability properties of the mixes using procedures proposed by Rangan (Rangan, 2008). A sodium silicate to sodium hydroxide ratio of 2.5 by mass was implemented as recommended by Mustafa et al. (Mustafa Al Bakri et al., 2012; Sanni & Khadiranaikar, 2012). The proportion of steel fiber was adjusted to 0.3% and 0.6% by volume. Ground granulated slag to fly ash ratio of three to one was used as a base material. The proportion of base materials (fly ash and slag) was adjusted based on the compressive strength of the trial mix. Detailed information on ten mix designs used in this experimental work is shown in Table 4.

The general mix procedures followed in this experimental work are explained below. Primarily, dry mixing of the base materials and aggregates was performed in a fixed pan mixer of 240-liter capacity with rotating blades existing in a construction materials laboratory and was continued for about 1 minute. Secondly, the activator liquids and superplasticizers were mixed into the dry mix for 2 minutes. After 2 minutes of mixing the solid constituents and liquid activators combined with superplasticizers in a pan mixer, steel fiber was manually distributed throughout the wet mix. Then, extra-water mixed with superplasticizer was added to the mix immediately after the fiber inclusion, and mixing continued for 1 minute until we obtained a homogeneous mix. Subsequently, the fresh geopolymer concrete was cast into the oiled cubical, cylindrical, and prismatic molds immediately after mixing. Specimens were vibrated on a vibration table for about 15s to remove air voids and leveled using a smooth trowel. Then after the

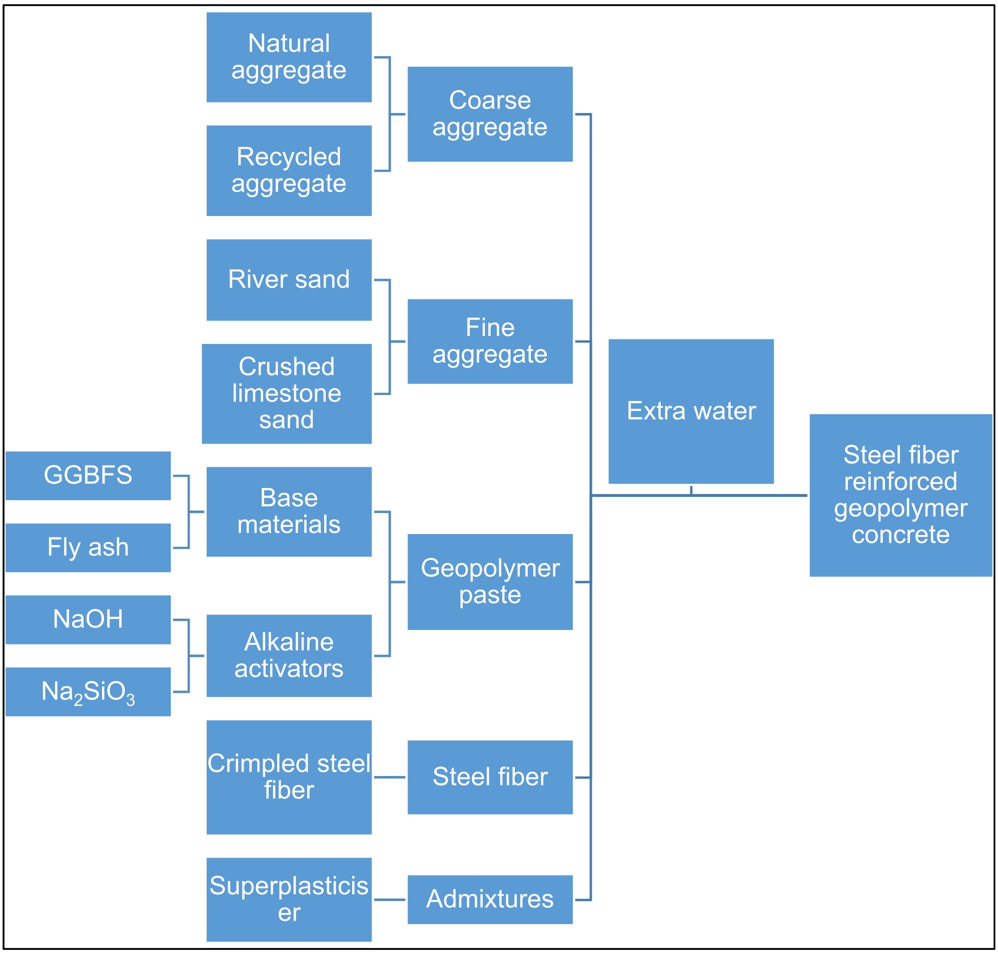

Figure 2. Steel fiber reinforced geopolymer concrete production process.

Table 4. The details of the mix proportion (kg/m^3).

Mix code	F.A.	Slag	NCA	RCA	RS	CS	NaOH	Na_2SiO_3	SP	EW	Steel fiber (By volume)
M1S3-0	89.54	268.63	1114.32	0	371.23	371.23	51.18	127.92	15.22	30.4	0.3%
M2S3-10	89.54	268.63	1002.8	111.44	371.23	371.23	51.18	127.92	15.22	30.4	0.3%
M3S3-20	89.54	268.63	891.44	222.88	371.23	371.23	51.18	127.92	15.22	30.4	0.3%
M4S3-30	89.54	268.63	780.02	334.30	371.23	371.23	51.18	127.92	15.22	30.4	0.3%
M5S3-40	89.54	268.63	668.58	445.76	371.23	371.23	51.18	127.92	15.22	30.4	0.3%
M6S6-0	89.54	268.63	1114.32	0	371.23	371.23	51.18	127.92	15.22	30.4	0.6%
M7S6-10	89.54	268.63	1002.8	111.44	371.23	371.23	51.18	127.92	15.22	30.4	0.6%
M8S6-20	89.54	268.63	891.44	222.88	371.23	371.23	51.18	127.92	15.22	30.4	0.6%
M9S6-30	89.54	268.63	780.02	334.30	371.23	371.23	51.18	127.92	15.22	30.4	0.6%
M10S6-40	89.54	268.63	668.58	445.76	371.23	371.23	51.18	127.92	15.22	30.4	0.6%

specimens were covered to restrict alkali liquid vaporization and kept at room temperature for 24 hours before demolding. Then after the test samples were removed from the mold and moved into the controlled curing room, the room's temperature was adjusted to 23 °C and relative humidity to 55 ± 10%. After the required age was attained, the specimens were removed from the curing room to wipe clean, and the test was taken.

3.2. Testing procedures

The 100 × 100 mm cubes, Φ100mm × 200 mm, 500 × 500 × 100mm prisms, and 71 × 71 × 71 mm prisms were cast. Immediately after molding, the specimens were covered to restrict alkali liquid vaporization and kept at room temperature for 24 hrs.; then, the test samples were demolded and moved into the controlled curing room adjusted to the temperature of 23 °C and relative humidity of 55 ± 10%. After the required age was attained, specimens were taken from the curing room to wipe clean, and intended tests were conducted.

A compressive strength test was conducted after 28 and 90 days using the 100 × 100mm cubes, and the test procedure was done according to EN 12390-3 (British Standard Institution BS EN 12390-3,3, 2009). The splitting tensile strength test was carried out after 28 and 90 days using the 100 × 200mm cylindrical samples according to the splitting tensile strength test procedure in ASTM C496 − 11 (ASTM C496-11,11, 2011). A flexural strength test was performed on 500 × 500 × 100mm prismatic specimens after 90 days of curing, according to ASTM C1609 (ASTM International. C1609/C1609M-12,12, 2012) standard procedure.

High-temperature, sulfate, and freezing-thawing resistance tests were also conducted using the 100 × 100mm cubic concrete samples to inspect the durability behavior of steel fiber-reinforced geopolymer concrete. Before and after these tests, an ultrasonic-pulse velocity (UPV) test was performed on the cubic specimens to inspect the effect of exposure conditions on the quality of the resulting concrete mixtures.

This study performed a series of experiments to investigate the temperature resistance of steel fiber-reinforced fly ash/slag-based geopolymer concrete produced with the partial replacement of recycled aggregate. The test samples were subjected to 200 °C, 600 °C, and 1000 °C in an electrically heated furnace after 90 days curing period at the rate of 5 °C/min in a vacuum atmosphere. Three different levels of temperature exposures are considered to observe the main physicochemical changes in the characteristics of concrete matrix caused by temperature elevations. As seen from previous literature, concrete responds differently to different temperature elevations. For instance, a temperature above 100 °C causes evaporation of physically accumulated water; the temperature within the range of 200 °C and 350 °C, mass loss occurs from the loss of water. On the other hand, at a temperature exceeding 350 °C, portlandite Calcium hydroxide starts to decompose, whereas, at an elevation higher than 700 °C, the de-carbonation of calcium carbonate happens (Bažant & Kaplan, 1996; Khoury, 2000; Neville, 1996).

Also, to facilitate the natural cooling process for the exposed specimens, the furnace was kept at the target temperature for one hour before it was turned off. The influence of the temperature was assessed based on observation, weight change, and compressive strength. However, the specimens subjected to a temperature of 1000 °C were only assessed based on their weight change. Furthermore, the UPV test was performed before and after exposing the specimens to the target temperature.

The sulfate resistance of the specimens was examined by determining the residual compressive performance, average variation in the specimen’s weight, and visual inspection. The 90 days concrete samples were soaked in the Magnesium Sulfate solution for two months. Magnesium sulfate solution with a 10% concentration was utilized as the standard exposure environment for all mixtures.

Each series of mixes were checked for freeze-thaw cycles and exposed to a total of 60. The test methodology for this test was done in compliance with ASTM C666 (1997) (ASTM, 1997). The freezing and thawing period was 24 hrs per cycle, with the temperature fluctuating between −18 °C to 4 °C. After 60 days of exposure, the specimens were removed from the testing machine, and their compressive performance difference and weight loss were computed about the specimens kept at room temperature. Also, the concrete specimen of 71 × 71 × 71mm was subjected to an abrasion test using a rotating disc abrasion machine. The specimen was centrally loaded with a 294 ± 3 N load. Each specimen was tested for 16 cycles, each consisting of 22 revolutions. The grinding path of the disc, evenly strewn with 20 g of the standard abrasive powder, rotates at a speed of 30 rpm. The thickness of the sample was measured using a thickness-measuring instrument from six points at the end of each cycle. Also, the resulting loss in mass of the specimen was evaluated to determine the concrete’s abrasion loss, using the specimen’s weight before and after each test. The abrasion thickness loss was evaluated after 16 cycles using the formula indicated in equation 3.5. Böhme test EN13892-3 (European Standard EN 1338, 1338, 2003) procedure was used to perform the abrasion test of the specimens.

$$t = \frac{M1 - M2}{M1} * \frac{V}{A} \tag{3.5}$$

Where:
t: Thickness loss due to abrasion (mm)

M1: Mass of the specimen before each test (g)
M2: Mass of the specimen after each test (g)
A: Surface area (50 cm^2) of the specimen in mm^2
V: Volume of the specimen in mm^3

The microstructure analysis of specimens was done using Scanning Electron Microscope (SEM) and FTIR spectroscopy. SEM test was performed at room temperature and after exposure to 200, 600, and 1000 °C. The specimens were randomly selected from the sections of the samples—the FTIR spectra of materials used in this study and some samples at 90-day age. Measurements were performed between 650 and 4000 cm^{-1}.

4. Results and discussion

4.1. Strength tests

4.1.1. Compressive strength test

According to Figure 3, the compressive strength results showed a slight improvement when the steel fiber percentage was raised from 0.3% to 0.6%. It might be related to the higher density of the steel fibers, which positively contributes to the strength development of the geopolymer concrete matrix. The enhancement originated essentially from the number of fibers encountering crack development. When the developing cracks reach the interface, the stress transfer will occur at the fiber matrix, allowing the fibrous composite specimens to resist additional compressive force, thus enhancing the mixtures' compressive performance with 0.6% over the 0.3% steel fiber. The strength decrement rate with the incorporation of RCA is higher in the case of 0.6% steel fiber addition compared to its corresponding mix design produced using a 0.3% fiber ratio. The compressive strength data given in Figure 3 shows that generally, the compressive performance of the samples was slightly decreased with the increase of recycled coarse aggregate ratio; however, the incorporation of 40% recycled coarse aggregate recorded the highest reduction rate of 22.61% and 21.05% in case of 0.6% and 0.3% steel fiber addition, respectively. The inclusion of 10%, 20%, and 30% RCA resulted in a 4.75%, 8.61%, and 13.63% reduction in the compressive performance of the concrete specimens prepared using 0.6% steel fiber content. According to Figure 3, the compressive strength of all the mixtures increased with the age increase from 28 to 90 days. The specimens gained most of their strength at the age of 28 days. Thus, only a slight rise was observed at 90 days. Behforouz et al. (Guo & Pan, 2018) studied the influence of RCA on geopolymer concrete and reported approximately identical reductions in the compressive strength with the incorporation of RCA Also, the negative effect of RCA on the compressive strength of concrete was reported by Nuaklong et al. (Ping & Yidong, 2011).

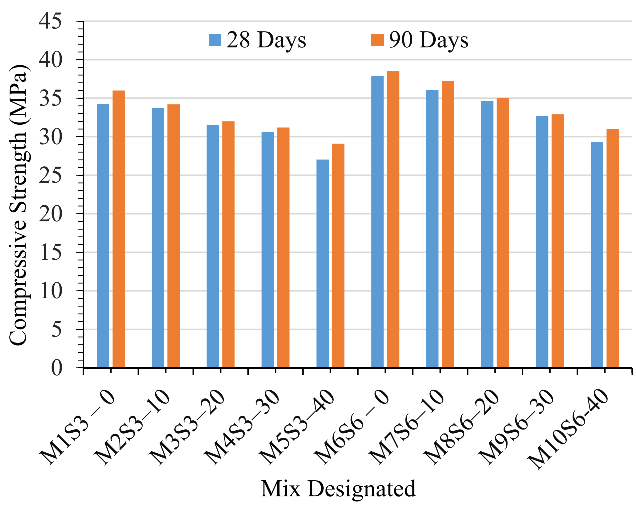

Figure 3. Compressive strength at the age of 28 and 90-days.

In conclusion, the compressive strength of geopolymer concrete produced with partial replacement of natural aggregates with recycled coarse aggregates was lower than that of natural aggregate concrete. It may be due to defects in recycled aggregates, more water added in recycled aggregates, and a weak interfacial zone between an old and a new cement matrix (Aguilar et al., 2010; Lee et al., 2018; Sata et al., 2013). The defects can lead to crack formation and low bond strength and thus decrease compressive strength. Regardless of the decrease in compressive strength, the substitution of 30% recycled coarse aggregates is adequately high for hiring in the construction industry. As a result, a proportion containing 0.6% steel fiber and 30% recycled aggregate can be considered an optimum mix design in terms of technical and environmental feasibility.

4.1.2. Tensile strength test

Tensile strength is among the vital properties of concrete, as concrete structures are highly susceptible to cracking. The tensile strength results of all specimens, as appeared in Figure 4, indicated approximately similar patterns to those of compressive strength.

As can be observed from Table 4, both 28 and 90 days tensile strength results of the concrete samples containing a steel fiber ratio of 0.6% possessed higher tensile strength results than that of 0.3%. For instance, the magnitude of 90 days splitting tensile Strength of M5S6-0 is higher (by approximately 15%) than its encounter with M1S3-0. The percentage rise for M7S6-10, M9S6-30, and M10S6-40 was recorded as 10%, 13%, and 12% compared to that of M2S3-10, M4S3-30, and M5S3-40, respectively. Approximately the same trend was observed for all the specimens tested at the age of 28 days. It demonstrates that adding fibers to the concrete mix improves the tensile performance of the resulting matrix (Gao et al., 1997). For instance, 0.6% of steel fiber resulted in a higher splitting tensile strength in comparison to 0.3% steel fiber incorporation. It is related to the fiber's ability to increase ductility and interrupt crack formation in concrete members, which increases with the fiber ratio up to its optimum content (Potrzebowski, 1983). Also, when the splitting happened and proceeded, the steel fibers connecting the divided parts of the composites acted through the load transfer from the concrete matrix to the fibers and, finally, the fibers received the entire load from the concrete matrix, and therefore the stress transfer enhanced the tensile strain potential of the 0.6% steel fiber more than its counter 0.3% fiber due to the higher number of fibers bridging the split portion in 0.6% fiber-reinforced composites. Thus, 0.6% of steel fiber addition improved the splitting tensile strength of the matrix over the concrete with a 0.3% fiber ratio. The statement agrees with the report by Potrebowski (Potrzebowski, 1983). Aamer Bhutta et al. (Bhutta et al., 2017) stated that the volume of fibers joining the fracture section directly affects the splitting tensile strength of fiber-reinforced concrete composites.

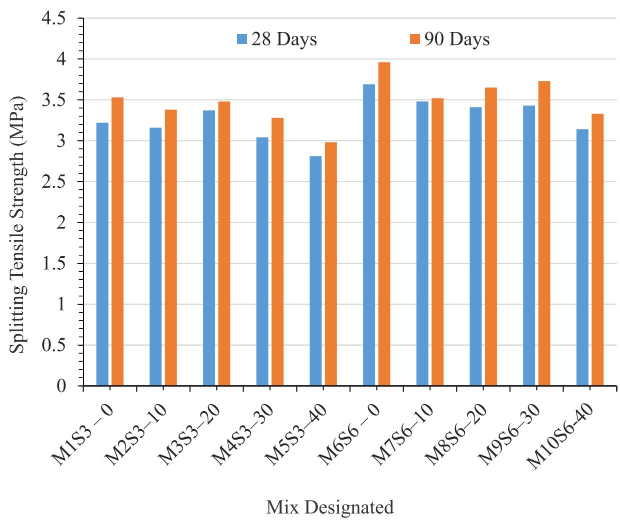

Figure 4. Splitting tensile strength at the age of 28 and 90-days.

At the 28 days strength, the application of 0.6% steel fiber without partial replacement of the recycled aggregate resulted in the highest splitting tensile strength. Incorporating 40% of RCA resulted in a maximum reduction rate of 14.90%, recorded as the most remarkable decrement rate throughout the mixtures produced. The RCA inclusion of up to 30% showed only a slight drop in the highest reduction, recording 7.58% and 5.59% of the reference specimen, in the case of 0.6% and 0.3% steel fiber ratio, respectively. As can be observed from Figure 4, the specimens' splitting tensile strength increased with age. The minimum and maximum increases were 3.4% and 9.7%, respectively. According to this study, the splitting tensile strength of the specimens was estimated as 9 to 10% of their corresponding compressive strength, which is approximately the same trend as that of conventional concrete.

In general, the splitting tensile strength of the samples was decreased with the increase of recycled coarse aggregate content. This is due to the porosity of recycled coarse aggregates and the weaker initiation of the interfacial transition zone (Ali et al., 2020; Thomas et al., 2018). Despite the fall in the tensile strength with the addition of recycled coarse aggregate, the replacement of 30% recycled coarse aggregates show a promising result for structural concrete production. Consequently, a mix incorporating 0.6% steel fiber and 30% recycled coarse aggregate can be used as an optimum mix design for both technical and environmental feasibility.

4.1.3. Flexural strength test

According to Figure 5, the mixtures produced without recycled coarse aggregate have a higher flexural strength value than those manufactured with recycled coarse aggregates, irrespective of the fiber content. It might be related to the low interfacial bond strength maintained between the new and old attached mortar. The finding agrees with the result of Padmini et al., 2009 (Padmini et al., 2009) and Nuaklong et al. (Nuaklong et al., 2016). The flexural strength of the specimens kept decreasing with the increase of the recycled coarse aggregate content in the case of 0.3% and 0.6% fiber ratio. The decrement rate was decreased with the increase of the recycled aggregate content, although the maximum fall in flexural strength occurred in concrete with an RCA proportion of 40%.

The increasing steel fiber content in the GPC matrix greatly enhanced flexural strength. The flexural strength of concrete mixtures produced without recycled aggregate and 0.6% steel fiber combined has increased by 30% compared to the specimens prepared with no recycled aggregate and 0.3% fiber ratio. Additionally, the flexural strength of the mixtures with 10%, 20%, 30%, and 40% partial replacement of recycled aggregate had increased by 32.57%, 29.04%, 3.13%, and 32.14%, respectively, when the fiber ratio increased from 0.3% to 0.6%. The flexural strength of all the specimens increased with the increase of age from 28 to 90 days.

In a nutshell, utilizing recycled coarse aggregate caused a reduction in the flexural strength of the concrete mix. However, the constructive contribution of steel fiber incorporation could overcome the drop in the flexural strength caused by the inclusion of RCA It is in line with the investigation performed by Prabu et al. (Prabua et al., 2017) and Behforouz et al. (Behforouz et al., 2020). Therefore, a concrete

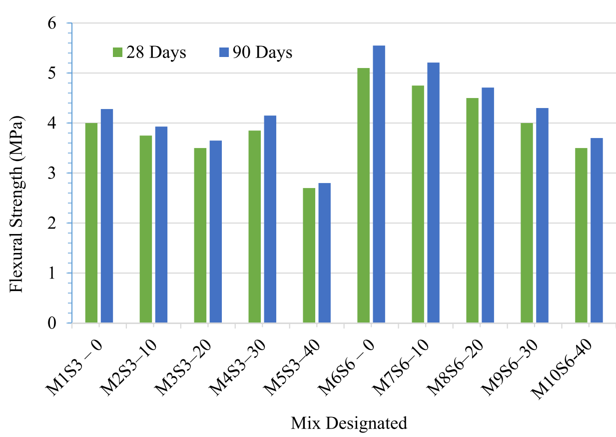

Figure 5. Flexural strength at the age of 28 and 90-Days.

mix produced from 30% RCA and 0.6% steel fiber can be considered an ideal proportion of engineering applicability and ecological feasibility, as observed in the compressive and tensile strength tests.

4.2. Abrasion resistance test

According to the results given in Table 5, the average wear of all the samples appeared to be less than 1 mm. M1S3-0 recorded an abrasion loss of around 0.61 mm, whereas M2S3-10, M3S3-20, and M4S3-30 experienced an average abrasion loss of 0.65 mm, 0.67 mm, and 0.69 mm, respectively. M5S3-40 saw an abrasion depth of around 0.72 mm, the highest abrasion loss throughout the ten mixes considered in this study.

On the other hand, the magnitude of wearing thickness for the mix identification M6S6-0 is registered as 0.47 mm, which is the lowest thickness loss in the given series of mixes. M7S6-10 and M8S6-20 saw a slightly higher abrasion loss, i.e., 0.5 mm and 0.52 mm, respectively. The abrasion thickness for M9S6-30 measured 0.54 mm. The magnitude of loss due to abrasion for M10S6-40 increased to 0.57 mm, the highest abrasion thickness measured for the concrete specimens produced using a steel ratio of 0.6%.

Generally, the wearing thickness and weight loss of the geopolymer concrete specimens increased with recycled coarse aggregate proportion. Nevertheless, the reduction rate for 0.3% steel fiber addition resulted slightly lower than its corresponding 0.6% steel-fiber ratio mix designs. The maximum increment in wear to the control specimen (Specimen without recycled aggregate) was recorded as 18.03% and 21.8% in the case of 0.3% and 0.6% steel fiber addition, respectively, at 40% recycled coarse aggregate replacement. The utilization of RCA in fly ash/slag-based geopolymer concrete resulted in a higher abrasion loss than a virgin aggregate concrete matrix. This statement is consistent with the investigation performed by Nuaklong et al. (Nuaklong et al., 2016).

Compared to 0.3% steel fiber inclusion, geopolymer concrete with a 0.6% steel fiber ratio recorded lower abrasion loss. It indicates that the matrix's abrasion resistance improved with an increased fiber ratio. It is due to the higher density of steel fiber reinforced geopolymer concrete specimens which were enhanced due to the better unit weight of steel fibers. Moreover, the fibers are short and randomly distributed throughout the mix, allowing them to arrest micro-cracks and minimize pores in a resulting concrete matrix. Ganesan et al. (Ganesan et al., 2015) revealed that the specimens with higher steel fiber content experienced the lowest thickness loss and therefore possessed a better abrasion resistance. It might be related to the enhanced density of steel fiber reinforced geopolymer concrete specimens because the fibers surrounded by the concrete would play a role of bridging micro-cracks and sometimes filling the small openings, which in turn reduces interconnecting pores to a minimum and leads to a lower weight loss and a higher abrasion resistance. As can be observed from the analysis, both abrasion depth and weight loss saw an increment with the rise of recycled aggregate content. However, the magnitude of wearing thickness and mass loss reduced with the increase of steel fiber ratio. As a result, the combined use of recycled coarse aggregate and steel fiber helps to improve the abrasive property of the geopolymer concrete matrix. Moreover, up to 30% partial replacement of recycled aggregate does not cause a significant reduction to control samples. These findings demonstrate that incorporating up to 30% RCA would be acceptable in applications and natural environment protection using recycled aggregate.

Table 5. Abrasion resistance test results.

Mix ID	Initial Weight (g)	Final Weight (g)	% weight loss	Average wear in (mm)	% increment in wear with respect to the control specimen
M1S3-0	822	818	0.49	0.61	control
M2S3-10	812	807.5	0.55	0.645	5.74
M3S3-20	808.5	803.5	0.62	0.67	9.84
M4S3-30	806.5	801	0.68	0.69	13.11
M5S3-40	802.5	796	0.81	0.72	18.03
M6S6-0	825.5	822	0.42	0.47	control
M7S6-10	816.5	812.5	0.49	0.5	6.38
M8S6-20	812.5	807.5	0.62	0.52	10.64
M9S6-30	797.5	792	0.69	0.54	14.89
M10S6-40	808	802	0.74	0.57	21.28

4.3. Ultrasonic pulse velocity test (UPV)

UPV test is a non-destructive test used to assess the homogeneity of the matrix and the dynamics in the structure of the mortar or concrete products. The concrete properties such as density, modulus of elasticity, and Poisson's ratio significantly affect the magnitude of the velocity of the ultrasonic pulse. According to Mouhcine et al. (Benaicha et al., 2015) ultrasonic pulse velocity test is illustrated as an appropriate method to determine the qualitative properties of concrete, such as the existence of defects, uniformity, and homogeneity of the matrix. It is, therefore, possible to determine the effect of temperature, freeze-thaw action, and sulfate attack on the resulting geopolymer concrete matrix using sonic evaluations.

From Figure 6, it is possible to note that incorporating recycled aggregates induces a reduction in UPV Also, it can be inferred that increasing fiber content does not provide a significant enhancement in UPV In the case of 0%, 10%, and 20% recycled aggregate ratio, there is only a slight improvement in the sonic velocity of the specimens with the increase of fiber content. Whereas the specimens produced with the addition of 30% and 40% recycled aggregate experienced a slight reduction in the UPV when the steel fiber ratio increased from 0.3% to 0.6%.

UPV decreased with the increase of recycled aggregate amount. For 10%, 20%, 30%, and 40% of recycled aggregate, the ultrasonic pulse velocity show reduction of 2.1%, 4.2%, 5.2%, and 6.2%, respectively, compared with non-recycled aggregate proportion (0% recycled aggregate) in the case of 0.3% fiber addition. Additionally, for 0.6% steel fiber, the magnitude of the ultrasonic pulse velocity dropped by 3.2%, 6.5%, 8.5%, and 10.4% compared with reference specimens to 10%, 20%, 30%, and 40% recycled aggregate incorporation, respectively. As mentioned above, ultrasonic velocity can be affected by the density and the level of uniformity of the resulting matrix. The sound velocity usually does not travel faster through liquid and gas. The concretes produced in this investigation include a different proportion of RCA; therefore, the inclusion of recycled aggregate at some level endowed the development of voids filled with air. As a result, the introduction of specific amounts of recycled aggregate reduced the sonic velocity of the mix due to its low density and some defects on the surface of RCA, which might lead to the formation of micro-cracks in the concrete matrix.

In a nutshell, the ultrasonic pulse velocity of the specimens decreased with the increase of recycled coarse aggregate; however, its magnitude saw a rise with the addition of steel fiber. This indicated that the incorporation of steel fiber has a constructive effect in improving the ultrasonic velocity of the resulting concrete matrix. Also, this property of the geopolymer concrete agrees with other strength properties indicated above. As a result, the synergetic effect of recycled coarse aggregate and steel fiber could improve the ultrasonic property of the concrete.

4.4. High-temperature resistance test

4.4.1. Compressive strength

The effect of high temperature on the residual compressive strength of the concrete samples manufactured with different proportions of RCA is given in Figure 7. The residual compressive strength of the

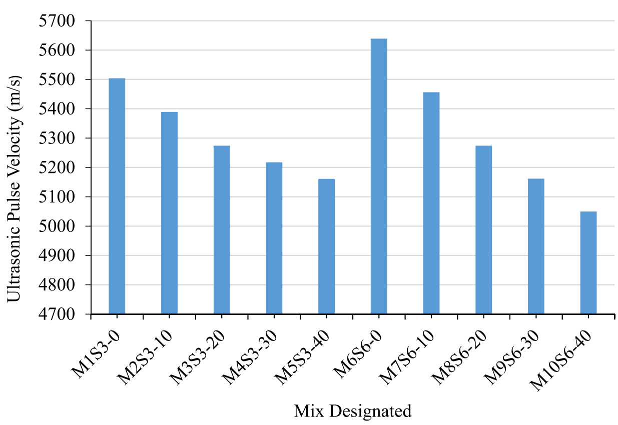

Figure 6. 90 days ultrasonic pulse velocity test result.

specimens is the ratio of strength at elevated temperature to that of ambient temperature. Results indicated that for all concrete specimens subjected to a temperature of 200 °C, the residual compressive strength improved in the range of 5-16% compared to their initial compressive strength at room temperature. The geopolymerization of base materials activated during heating contributes to the strength behavior, and therefore a continuation of geopolymerization has resulted in a strength gain at this temperature. The performance improvement character of the geopolymeric products after the elevated temperature exposure was also reported in the previous studies by Abdulkareem et al. (Abdulkareem et al., 2014). The steel fiber added might be partly responsible for the possible enhancement of the resulting strength (Novák & Kohoutková, 2017). The residual compressive performance of the concrete mixtures is reduced as the temperature rises from 200 °C to 600 °C. For instance, the N.C.A. concrete mixtures fabricated with a steel ratio of 0.3% and 0.6% have experienced a compressive strength loss of 7.5% and 10%, respectively, after being subjected to a temperature of 600 °C, whereas the concrete specimens with RCA had a compressive strength loss of 13-21% compared to their initial strength at an average temperature. Moreover, the mixtures containing a higher ratio of steel fiber have experienced lower strength change after exposure temperatures of both 200 °C and 600 °C.

The residual compressive strength of the control samples recorded a higher magnitude than that of the mixtures produced with recycled aggregates after exposure to elevated temperatures of 200 °C and 600 °C. When the geopolymer concrete was subjected to an elevated temperature of 1000 °C, the decomposition of coarse limestone aggregate and that of limestone crushed sand led to structural failure due to the deterioration caused by the expansion of burnt limestone products (Junru et al., 2019). Additionally, the thermal incompatibility among aggregates and cement paste which can cause interconnected cracks at the interfacial zone of the geopolymer concrete matrix, can be a possible reason for the concrete matrix disintegration at this temperature (Sarhat & Sherwood, 2013; Yan et al., 2007).

It can be inferred that even though there was a decrease in compressive strength due to recycled coarse aggregate, the inclusion of steel fiber can encounter strength loss due to the recycled aggregate. The possible reason for the reduction of strength loss with the increase of steel fiber ratio may be related to the ability of fibers to limit the spread of cracking, potentially enhancing the performance of concrete matrix after being subjected to elevated temperature. This trend agrees with the study by Hannant D.J (Hannant, 1978). As a result, the combined use of recycled coarse aggregate and steel fiber would significantly produce structurally fit fiber-reinforced geopolymer concrete using recycled coarse aggregate.

4.4.2. Mass loss

Figure 8 demonstrated that at any specified temperature, the weight loss in reference specimens (M1S3-0 and M6S6-0) was lower than that of the specimens produced with the incorporation of the recycled aggregate. Moreover, the reduction rate was slightly increased with the recycled aggregate ratio, which was attributed to a higher amount of water released from the recycled coarse aggregate because recycled aggregate possesses a higher water absorption capacity than natural aggregate. The same result

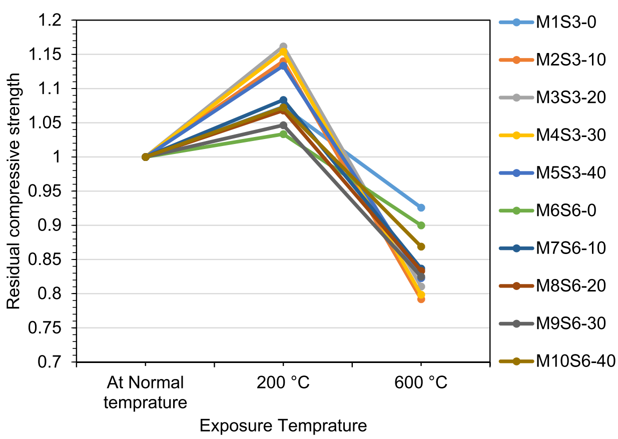

Figure 7. Residual compressive strength.

was reported in the study by Lanyerie et al. (Laneyrie et al., 2016). The maximum weight loss at 200 °C, 600 °C, and 1000 °C was recorded as 2%, 10%, and 14% of the specimens at an average temperature. As mentioned in the previous section, both recycled and natural aggregates were moisturized to maintain the aggregates' surface saturated state based on the aggregate type's water absorption capacity. As a result, the mixes with recycled aggregates contain higher water content than virgin aggregate concrete mixes. It can also be seen that the rate of weight loss from 200 °C to 600 °C has dramatically increased for nearly all concrete mixtures. In the study by Duxson et al. (Duxson et al., 2007), it was illustrated that a couple of effects known as dihydroxylation and water evaporation are identified as the main contributors to the weight loss of the geopolymer matrix at elevated temperatures. The type of water in a dried geopolymer matrix can be physical, chemical, or hydroxyl.

Moreover, each type of moisture evaporates at a distinct temperature range. For instance, the hydroxyl group departs at temperatures exceeding 300 °C, whereas the chemical and physical ones depart at 100 ∼ 300 °C and 20 ∼ 100 °C, respectively. Therefore, the abrupt mass loss from 200 °C to 600 °C might be due to the complete occurrence of both dihydroxylation and water evaporation. At 600 °C and 1000 °C, both the magnitude of mass loss and the rate of mass loss showed a slight increment with the increase of the fiber content; at a temperature higher than 750 °C geopolymer concrete matrix experiences the decomposition of carbonate species which leads to to the weakening of interfacial bond strength of the resulting matrix (Rakhimova et al., 2018). Therefore, the decomposition of carbonate families can cause the highest weight loss at 1000 °C.

On the other hand, no significant change in weight loss percentage was observed with the variation of steel fiber ratio. For instance, the mass loss percentage for M1S3-0 and M1S6-0, after being exposed to 600 °C, is recorded as 4.6 and 4.4, respectively. As a result, the combined effect of recycled coarse aggregate and steel fiber has little or no impact in terms of weight loss.

4.4.3. Ultrasonic pulse velocity

Figure 9 shows the ultrasonic pulse velocities of mixtures with and without recycled aggregate subjected to an elevated temperatures of 200 °C and 600 °C. Figure 9 shows that the specimens manufactured without recycled aggregate resulted in a higher magnitude of the ultrasonic pulse velocity in the case of 0.3% and 0.6% steel fiber content.

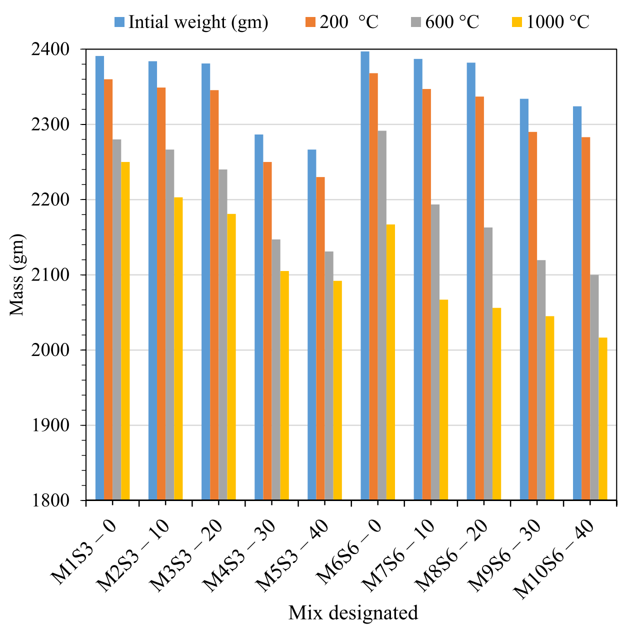

Figure 8. Weight of the specimens before and after exposure to elevated temperature.

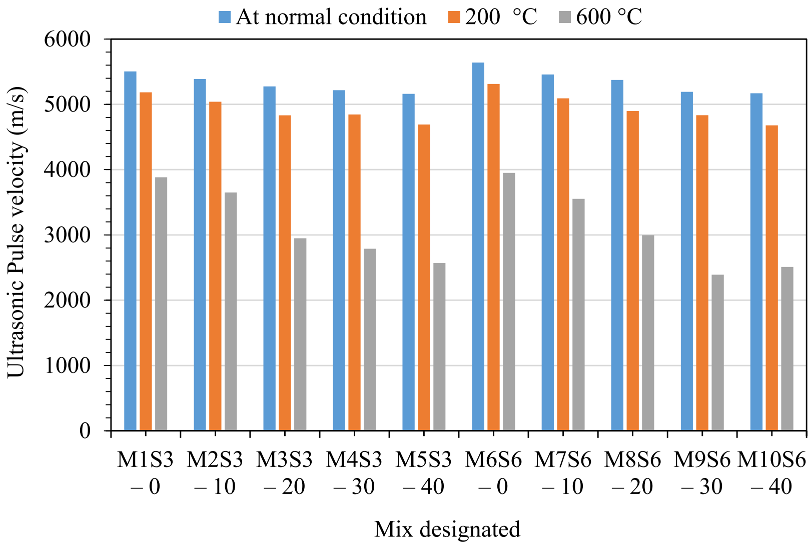

Figure 9. Measured UPV of specimens before and after exposure to elevated temperature.

Moreover, at any target temperature, all mixtures' ultrasonic pulse velocity values dropped with the rise of recycled aggregate content. However, a change in the content of the fiber does not cause a significant effect on the magnitude of ultrasonic pulse velocity. At 200 °C, a drop in ultrasonic pulse velocity was 8.5%. It might be related to less or no development of defects such as cracks and pores during this heat exposure. Nevertheless, when the heat intensity grows to 600 °C, the pulse velocity significantly drops with a minimum and maximum reduction rate of 29.5% to 53%, respectively. It may be attributed to the higher crack width and significant weight loss, which results in a reduced density of the specimens. Furthermore, the defects in the geopolymer concrete specimens were raised seriously as the sample was subjected to a high temperature of 1000 °C. After the standing time of 3 days in the curing room, the specimens exposed to 1000 °C become inappropriate for conducting the ultrasonic pulse velocity and compressive strength, as shown in Figure 10.

In conclusion, the ultrasonic pulse velocity of the concrete specimens saw a decline with the temperature increase. Moreover, the specimens containing a higher percentage of recycled coarse aggregate possessed low ultrasonic pulse velocity. However, the steel fiber ratio variation does not show an essential change in the ultrasonic pulse velocity of the resulting concrete matrix.

4.4.4. Physical observation

Figure 10 illustrate the physical appearance of the subjected and unexposed geopolymer concrete specimens to the high temperatures of 200 °C, 600 °C, and 1000 °C, consecutively. It can be observed that the specimens undergo a color change, corner breakages, and cracks which appear worse with the temperature rise. The concrete specimens exposed to 1000 °C experienced the highest thermal crack distribution and width. Moreover, the decomposition of the concrete matrix was observed, resulting in breakage and spalling. The coarse aggregates after the target temperature of 1000 °C altered to white and light yellow. It might be due to the decomposition of limestone coarse aggregates after an elevated temperature of 1000 °C (Prabua et al., 2017). After the cooling period of 3 days, the coarse aggregates have highly deteriorated. The decomposition of coarse aggregates and vast distribution of cracks led to the failure of the concrete structure without any induced load; as a result, it was not possible to conduct ultrasonic pulse velocity and compressive strength tests (Figure 10 (e)).

The visual appearance change was seen in all specimens irrespective of the proportion of the ingredients. The color of specimens subjected to 200 °C, 600 °C, and 1000 °C changed to dark gray, light red, and light yellow, respectively. It is characterized by the oxidation changes derived from ferric oxide content in fly ash/slag-based geopolymer (Ganesan et al., 2015).

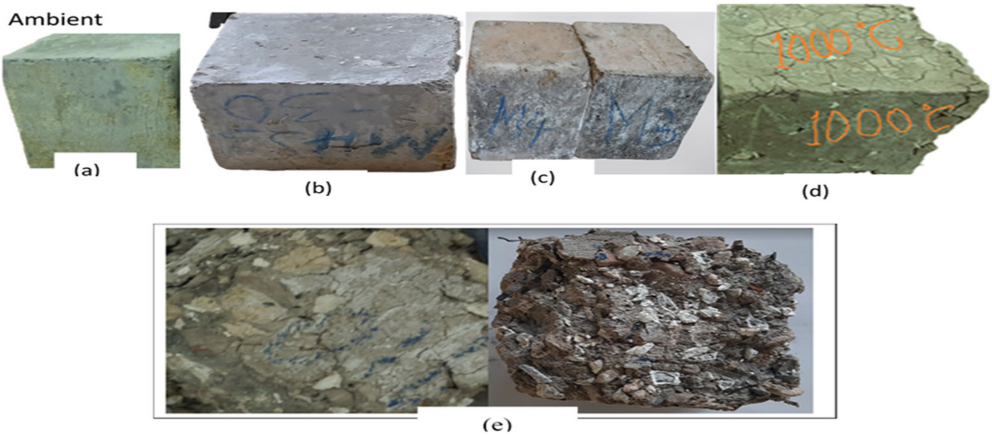

Figure 10. Surface changes of the specimens after exposure to temperature. (a). Ambient temperature (b). After 200 °C (c). After 600 °C (d). After 1000 °C (e), Specimens were exposed to 1000 °C after waiting in the curing room for three days.

As can be seen from Figure 10, no significant change was observed due to the synergetic effect of recycled coarse aggregate and steel fiber, although a change in the color of the concrete specimens was seen with the rise of elevated temperature.

4.5. Sulfate resistance test

Chemical attack is among the severe problems for concrete that can deteriorate the concrete matrix's physical, chemical, and mechanical properties (Arafa et al., 2017; Chabrelie, 2010). In this experimental work, the resistance to chemical attack of concrete samples was evaluated by performing a magnesium sulfate test. The influence of sulfate on the physical appearance, strength characteristics, mass change, and ultrasonic pulse velocity was assessed. The physical appearance of the concrete samples after being immersed in a 10% sulfuric acid solution for 60 days showed no significant change in the appearance of the subjected samples. No specimen has shown the effect of surface deterioration or spalling. However, the specimens produced from 100% natural aggregate experienced some signs of surface cracking and small voids. The magnesium sulfate resistance test's outcomes appear in Figures 11–13. The maximum mass gain experienced by 0.3% of steel fiber incorporation was 4%, whereas, for 0.6%, it was 4.7%. When the geopolymer concrete samples are exposed to sulfate solution, the calcium and aluminum phase in geopolymer products could react with the SO_4^{2-} in the solution to give $CaSO_4$ and ettringite, which improves the density of the concrete matrix, and therefore this results in a weight gain (Xie et al., 2019). For 0.3% and 0.6% of steel fiber addition, a percent of mass gain was increased with the increased recycled aggregate ratio. The rise in mass with the increase of recycled coarse aggregate content might be related to the recycled aggregates possessing a higher volume of pores to safeguard newly occurred minerals from acid attack (Xie et al., 2019). However, further stay (more than two months) in the sulfuric environment might have decreased the weight of the specimens produced with recycled aggregate due to the weaker microstructure of the recycled aggregate. The compressive strength of the concrete mixtures has shown both rise and fall after exposure to sulfate attack. Incorporating the recycled coarse aggregate ratio of 20%, 30%, and 40% has resulted in a gain in compressive strength, whereas 0% and 10% have experienced a minimal loss in their compressive performance. The possible cause for the increase in the samples' compressive strength could be the denser microstructure due to the formation of calcium sulfate and ettringite in the initial SO_4^{2-} attack, which might help the filling of the micro-pores. Veerendra Babu et al. (Babu et al., 2017) also reported the rise in the compressive strength of the geopolymer concrete specimens exposed to magnesium sulfate. After being exposed to sulfate attack, the ultrasonic pulse velocity of the specimens was increased with the increase of recycled coarse aggregate and fiber ratio. The rise in the magnitude of ultrasonic pulse velocity went hand in hand with weight gain because of the reason mentioned above. The maximum ultrasonic pulse velocity increase for 0.3% and 0.6% of steel fiber volume was 5.81% and 6.38%, respectively.

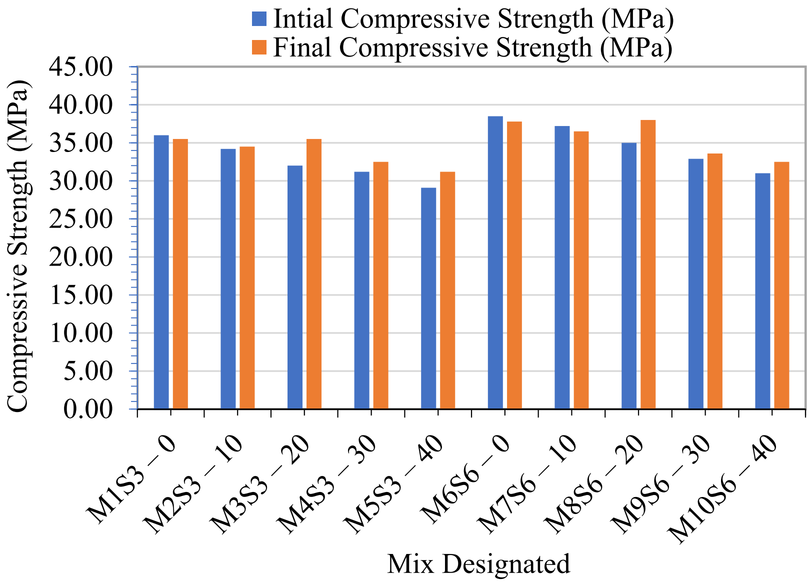

Figure 11. Specimens of compressive strength before and after sulfate attack.

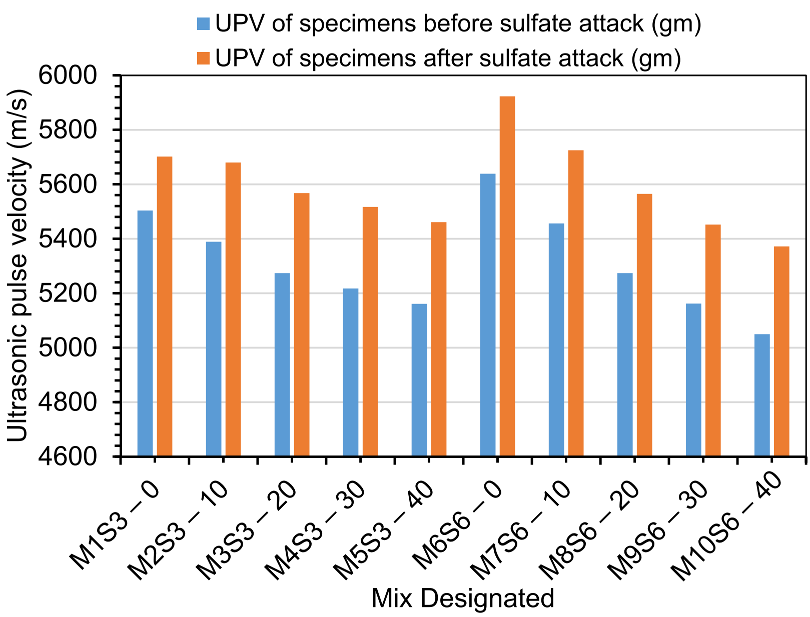

Figure 12. Ultrasonic pulse velocity before and after the sulfate attack.

4.6. Freezing-thawing resistance test

This study used changes in compressive strength, weight, and ultrasonic pulse velocity magnitude change to assess the impact of freezing-thawing on the geopolymer concrete mixtures. Test results indicated that 0.3% and 0.6% of steel fiber-reinforced geopolymer concrete mixtures suffered insignificant mass reduction and less than a 10% decrease in compressive performance. The minimal weight loss is mainly related to the concrete surface and edge defects due to the freezing and thawing effects. It can also be observed from Figure 14 that the specimens produced with the partial replacement of recycled coarse aggregate have resulted in a lower weight than that of the specimens prepared from 100% natural aggregate. The mixtures with 40% recycled coarse aggregate have experienced the maximum loss in

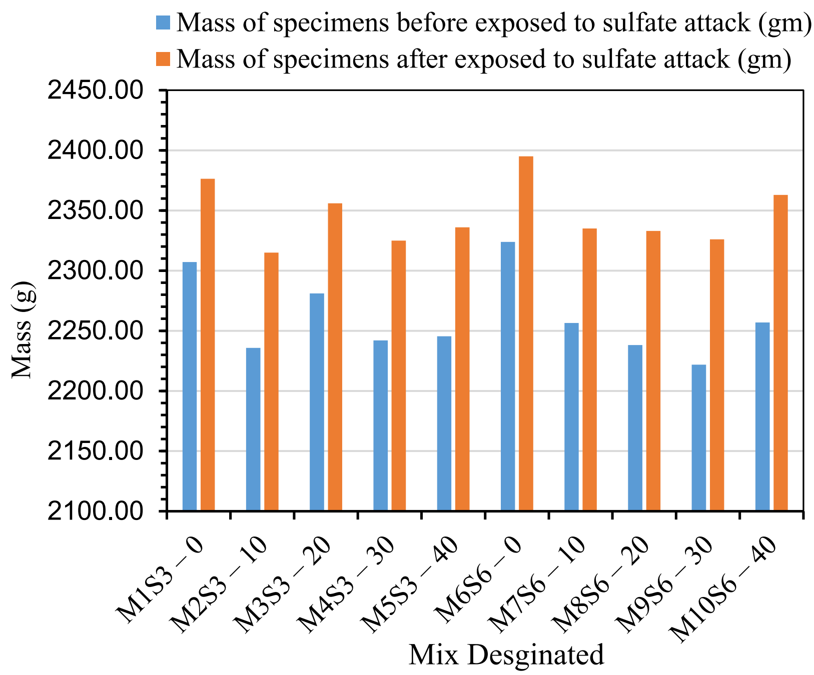

Figure 13. Weight of specimens after and before exposure to sulfate attack.

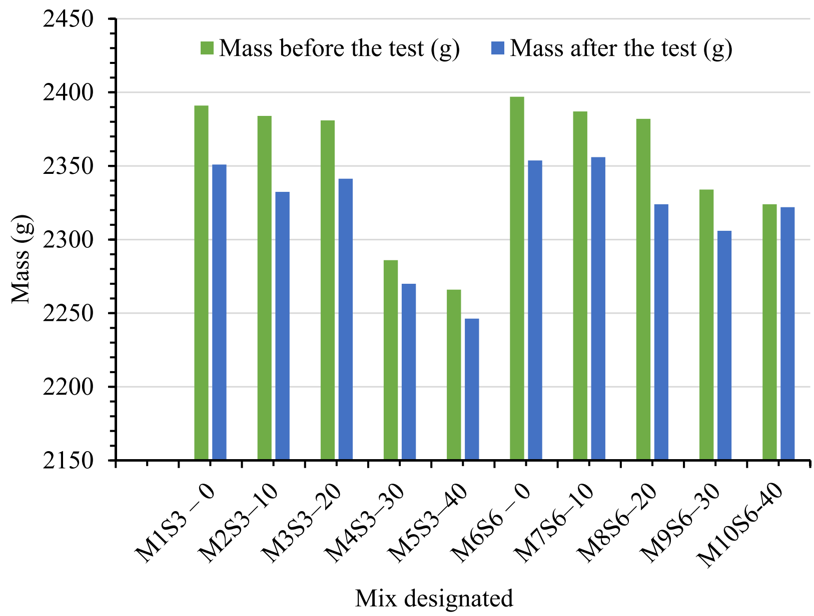

Figure 14. Weight of specimens after and before exposure to freeze-thaw.

compressive strength. The loss in compressive strength was reduced with the increase in fiber content. As was observed in previous sections, the reduction in compressive strength caused due to the inclusion of recycled aggregate shall be compensated by adding fibers to the concrete mixture. As can be observed from Figure 15, the concrete mixtures with recycled concrete aggregates resulted in a lower compressive strength than the control specimens. However, the rate of reduction is not statistically significant. The possible reason is the effect of freezing and thawing in the concrete can be expressed in

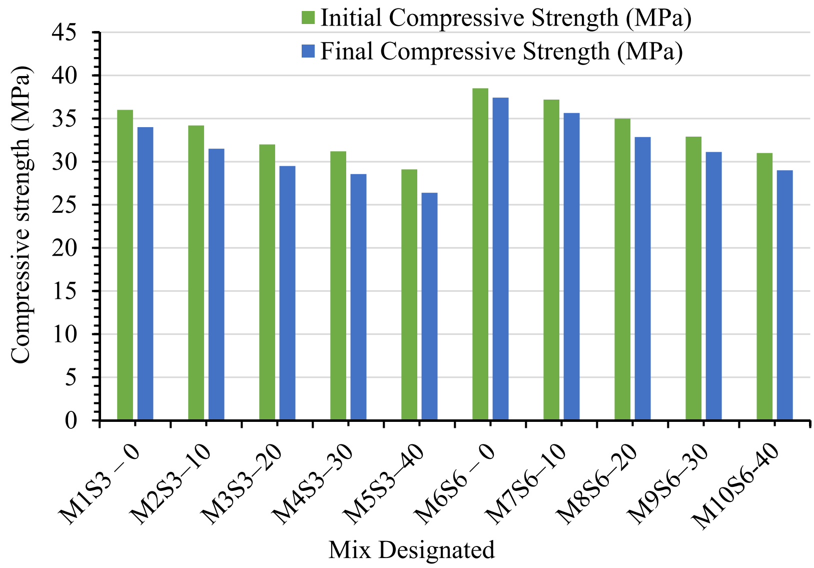

Figure 15. Compressive strength before and after exposure to freeze-thaw.

terms of matrix and aggregate. Primarily, the freezing and thawing effect on the matrix is based on the interconnected voids and saturation level of concrete, which can be interrupted by the addition of fibers, whereas the effect on the aggregates relates to the porosity of aggregates which can be mitigated with the incorporation of dense matrix (Ganesan et al., 2015). In this study, the synergetic effect of fibers and dense matrix such as slag has enhanced the freezing and thawing resistance of the steel fiber-reinforced geopolymer concrete specimens. Due to that, the specimens showed better performance against the freezing and thawing effect. The ultrasonic pulse velocity of the concrete samples shown in Figure 16 also has the same trend as that of the compressive strength and weight of the specimen.

5. Microstructural analysis

5.1. Scanning electron microscope (SEM)

The SEM images of M5S3-40 and M10S6-40 specimens at 25, 200, 600, and 1000 °C are presented in Figures 17 and 18. SEM was conducted to analyze the microstructures of specimens made with 40% (highest ratio) replacement of natural aggregate with RCA with different fiber ratios of 0.3% and 0.6% at elevated temperatures. Steel fiber reinforced geopolymer concrete mixtures demonstrates homogenous and highly compact microstructure at 25 °C. As observed, with an increase in the temperature up to 200 °C, some cracks can be seen in M5S3-40, while there seem to be fewer cracks in M10S6-40 which can be attributed to the presence of steel-fiber. However, the samples were able to gain more strength at 200 °C.

As indicated in Figures 17 and 18, the crack growth rates increase at 600 °C. In addition, the initial crack's propagation seems to be faster in M5S3-40. The M10S6-40 contains more steel fiber which can act like a bridge and prevent and limit cracks. Furthermore, the interface zone between the aggregate and the paste has been lost in some parts of the M5S3-40, which can reduce the strength of the concrete samples. Besides, the thermal expansion of the aggregates led to cracks in the past due to internal stresses (Plank & Winter, 2008). These observations explain the low values of the residual compressive strength.

At a temperature of 1000 °C, many parts of both samples have deteriorated because heat and concrete are not structurally valid. In such high temperatures, spalling can occur, but a higher steel fiber ratio in M10S6-40 increases strength significantly and can enhance resistance against spalling. The high porosity of the samples at 1000 °C can probably be due to the harder escaping of water from a mortar at high temperatures, which can justify the mass loss results. The results were in complete agreement with previous findings.

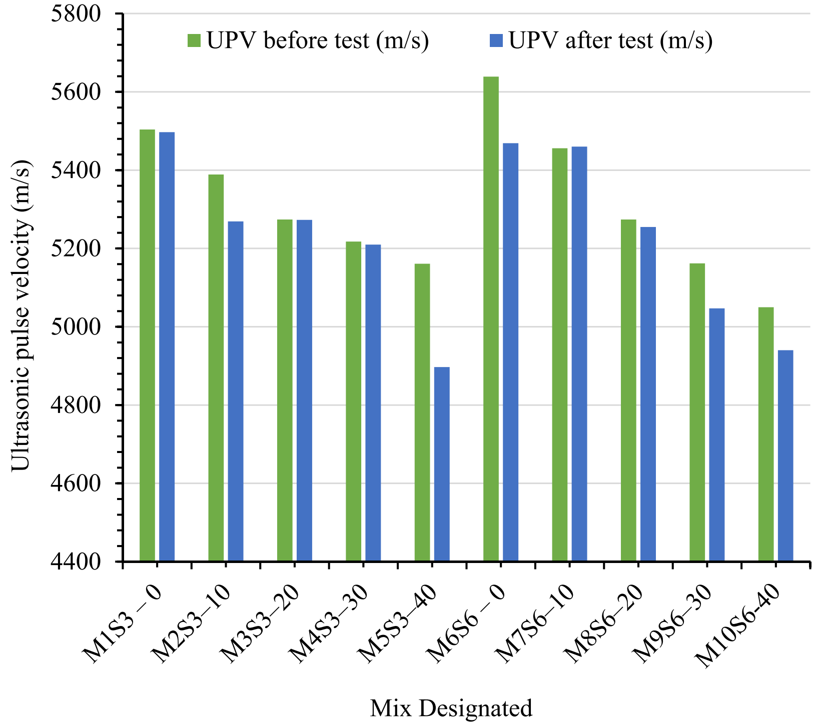

Figure 16. Ultrasonic pulse velocity before and after the freeze-thaw test.

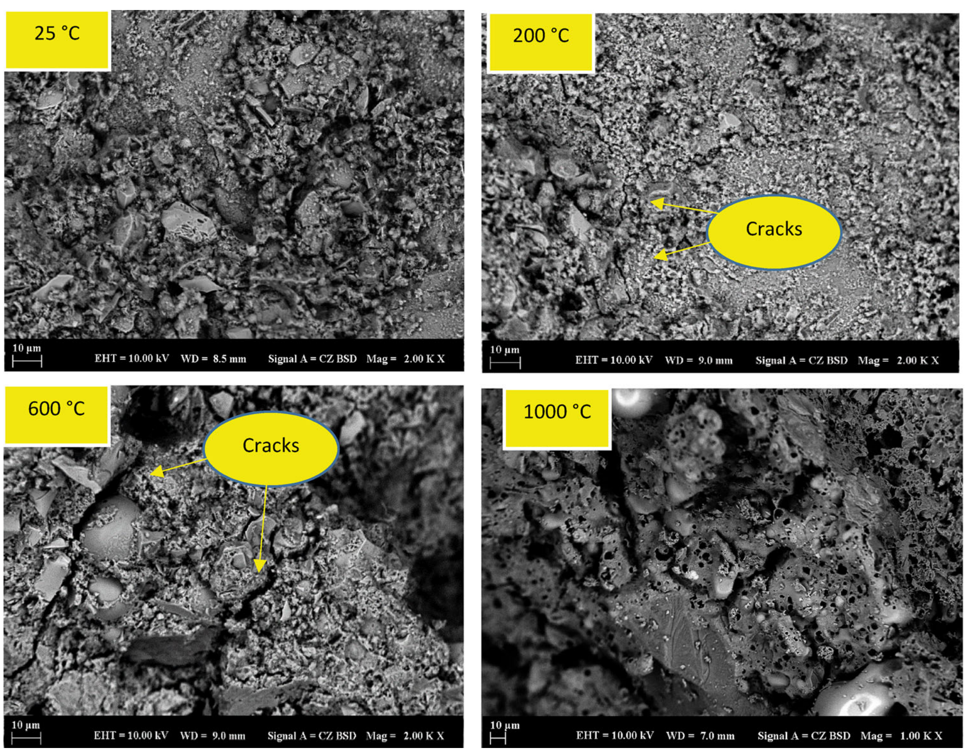

Figure 17. SEM images of M5S3-40 at different temperatures.

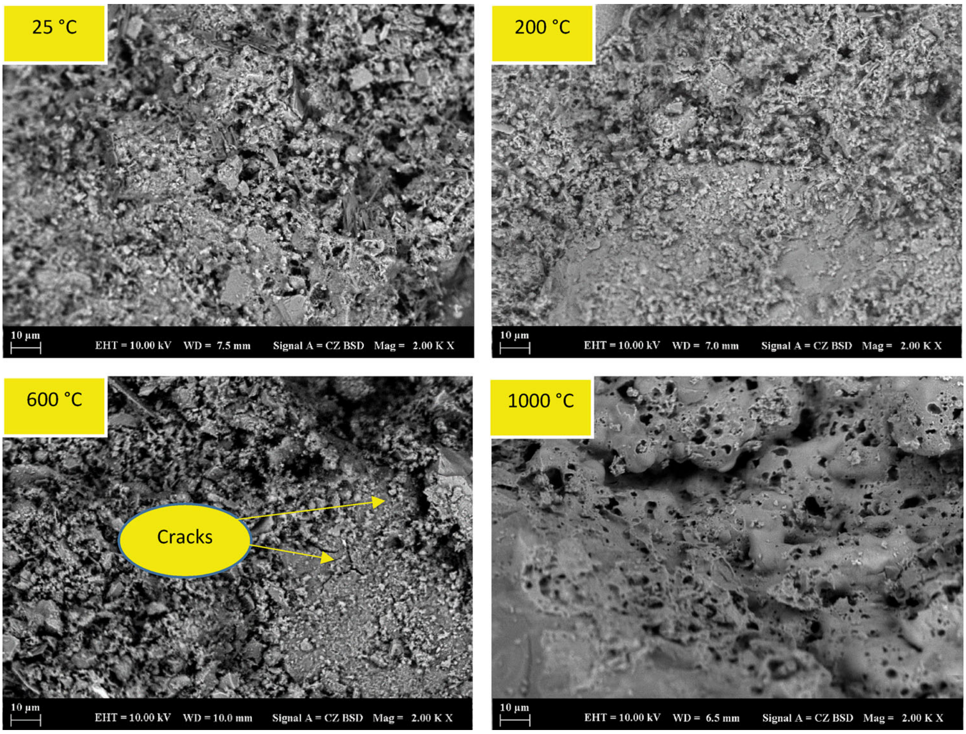

Figure 18. SEM images of M10S6-40 at different temperatures.

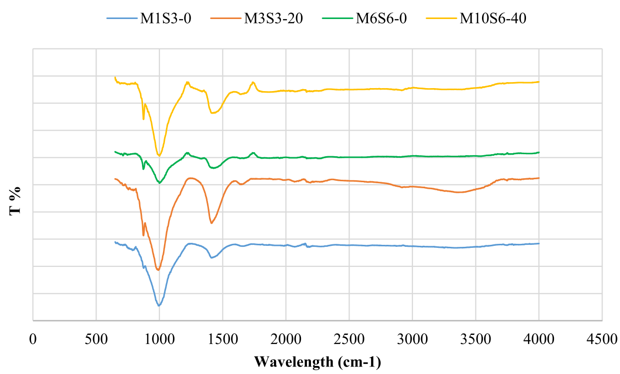

Figure 19. The results of the FTIR analysis.

5.2. Fourier transform infrared spectroscopy (FTIR)

The FTIR analysis results of four specimens between 600 and 4000 cm-1 are presented in Figure 19. As can be seen, all samples showed identical bands representing the same hydration products independent of the amount of fiber and RCA In each geopolymer matrixes spectra, a similar peak appears at 874, 992, and 1417 cm^{-1}. The peak identified at 874 and 1417 cm^{-1} suggests the presence of CO_3^{2-}, which can be related to, the presence of calcite or hydrotalcite that might be formed from the remaining unreacted activator. The appearance of bands at ~992 cm^{-1} probably relates to the Si-O asymmetric stretching bands in Q2 units. It is generally accepted that the v_3 (Si-O) bond stretching vibration in the I.R. spectra of C-S-H gels is at 950-994 cm^{-1}. Based on what was reported by Garcia-Lodeiro et al. (García-Lodeiro et al., 2011) and Rees et al. (Rees et al., 2007), the peak identified at 992 cm^{-1} is in line with the structure of both the C-(A)-S-H and the N-A-S-H gels. The results have several similarities with Abdalqader et al.

(Abdalqader et al., 2016) findings. In addition to all the above peaks, the small bands at 1650 cm^{-1} can be related to the water molecules occluded inside the aluminosilicate structure (Gök et al., 2007).

6. Conclusions

The main goal of this study is to produce fiber-reinforced geopolymer concrete where recycled coarse aggregate is used as a partial substitute for natural coarse aggregate with better strength and durability properties. Among several construction and demolition wastes, recycled coarse aggregate holds a significant share of the total waste worldwide. Also, using recycled aggregate helps reduce the consumption of virgin aggregate and improve sustainability; therefore, it would have a significant role in maintaining the balance of a natural ecosystem. Thus, it is essential to study the feasibility of recycled aggregate in combination with a steel fiber for utilization in concrete production. In this study, the synergetic effect of steel fiber and recycled coarse aggregate on the mechanical and durability properties of steel fiber reinforced fly ash/slag-based GPC manufactured with the partial replacement of recycled aggregate were addressed, and the following conclusions were drawn.

- The strength properties of the concrete reduced with the rise of recycled aggregate content. This may be due to defects in the recycled aggregates and the weak bond formed between an old, attached mortar and a new mortar formed from fly ash and slag. On the other hand, the compressive strength, splitting tensile strength, and flexural Strength of all the mixtures were improved when the fiber content rose from 0.3% to 0.6%. Furthermore, the influence of including fibers on the compressive performance (rise within the range of 6 to 9%) and splitting tensile strength (rise within the range of 4 to 12%) is less, but the flexural strength saw a significant change (up to 32% increase) when the steel fiber content increases from 0.3% to 0.6%.
- When subjected to a temperature of 200 °C, the compressive strength of all the specimens compared to the original strength was increased irrespective of the aggregate type. While at 600 °C, the specimens manufactured with recycled aggregate started losing their original strength. The maximum reduction recorded 21% of the initial compressive strength, seen in the specimen prepared with 30% recycled aggregate and 0.3% steel fiber content. The strength loss of the specimens subjected to elevated temperature experienced a rise with the incorporation of recycled coarse aggregate. However, the concrete specimens that added 0.6% steel fiber possessed higher residual compressive strength than those obtained by hiring 0.3% steel fiber. This is due to the ability of the fibers to restrain crack development and propagation. As a result, the combined use of recycled coarse aggregate and steel fiber has a constructive effect on the compressive strength of the resulting geopolymer concrete matrix.
- The specimen's ability to resist the abrasion effect was prospective. In this study, the concrete mixtures subjected to the abrasion test suffered less than 1m abrasion loss. The wear thickness was increased with the increase of the recycled aggregate content. However, it was reduced with the increase of fiber content from 0.3% to 0.6%. This confirms the synergetic effect of steel fiber and recycled coarse aggregate.
- The overall freezing-thawing resistance of fly ash/slag-based geopolymer concrete with partial incorporation of recycled aggregates was approximately like that of the specimens produced with natural aggregates only. According to the findings from the study, an insignificant effect was observed in the freezing-thawing resistance parameters with the increase of fiber content. After being exposed to sulfate attack, all the specimens gave higher compressive strength, weight, and ultrasonic pulse velocity magnitude compared to their original property before being subjected to this environment.
- The specimens with the addition of RCA of up to 30% and 0.6% steel fiber possessed good overall properties. However, the strength properties of the specimens were decreased with the increase of recycled coarse aggregate ratio.

Disclosure statement

No potential conflict of interest was reported by the author(s).

Funding

This work was supported by the research fund of the Yildiz Technical University, and the authors would like to express their sincere gratitude to the Scientific Research Coordination unit for their financial support of the project (Project number: FBA-2019-3558).

Data availability statement

Data available on request from the authors.

References

Abdalqader, A. F., Jin, F., & Al-Tabbaa, A. (2016). Development of greener alkali-activated cement: utilisation of sodium carbonate for activating slag and fly ash mixtures. *Journal of Cleaner Production*, *113*, 66–75. https://doi.org/10.1016/j.jclepro.2015.12.010

Abdulkareem, O. A., A., Bakri, A. M., Kamarudin, H., Nizar, I. K., & Ala'eddin, A. S. (2014). Effects of elevated temperatures on the thermal behavior and mechanical performance of fly ash geopolymer paste, mortar and lightweight concrete. *Construction and Building Materials*, *50*, 377–387. https://doi.org/10.1016/j.conbuildmat.2013.09.047

Aguilar, R. A., Díaz, O. B., & García, J. E. (2010). Lightweight concretes of activated metakaolin-fly ash binders, with blast furnace slag aggregates. *Construction and Building Materials*, *24*(7), 1166–1175. https://doi.org/10.1016/j.conbuildmat.2009.12.024

Ali, A. A. M., Zidan, R. S., & Ahmed, T. W. (2020). Evaluation of high-strength concrete made with recycled aggregate under effect of well water. *Case Studies in Construction Materials*, *12*, e00338. https://doi.org/10.1016/j.cscm.2020.e00338

Arafa, M., Tayeh, B. A., Alqedra, M., Shihada, S., & Hanoona, H. (2017). Investigating the effect of sulfate attack on compressive strength of recycled aggregate concrete. *Journal of Engineering Research and Technology*, *4*(4), 66–77. https://publisher.uthm.edu.my/ojs/index.php/IJSCET/article/view/1746

ASTM C496-11. (2011). Standard test method for splitting tensile strength of cylindrical concrete specimens. In *Annual* Book of ASTM *standards* (vol. *4*, pp. 1–5).

ASTM C618-19. (2019). *Standard specification for coal fly ash and raw or calcined natural pozzolan for use in concrete*. ASTM International.

ASTM International. C1609/C1609M-12. (2012). *Standard test method for flexural performance of fiber-reinforced concrete (using beam with third-point loading)*.

ASTM. (1997). *Standard test method for resistance of concrete to rapid freezing and thawing. ASTM C666*. ASTM.

Babu, N. V., Rahul, B. G., & Kumar, Y. H. (2017). Experimental study on strength and durability properties of GPC with GGBS. *International Journal of Civil Engineering and Technology*, *8*(4), 39–50.

Bažant, Z. P., & Kaplan, M. F. (1996). *Concrete at high temperatures: Material properties and mathematical models*. Longman.

Behforouz, B., Balkanlou, V. S., Naseri, F., Kasehchi, E., Mohseni, E., & Ozbakkaloglu, T. (2020). Investigation of eco-friendly fiber-reinforced geopolymer composites incorporating recycled coarse aggregates. *International Journal of Environmental Science and Technology*, *17*(6), 3251–3260. https://doi.org/10.1007/s13762-020-02643-x

Ben Nakhi, A., & Alhumoud, J. M. (2019). Effects of recycled aggregate on concrete mix and exposure to chloride. *Advances in Materials Science and Engineering*, *2019*, 1–7. https://doi.org/10.1155/2019/7605098

Benaicha, M., Jalbaud, O., Alaoui, A. H., & Burtschell, Y. (2015). Correlation between the mechanical behavior and the ultrasonic velocity of fiber-reinforced concrete. *Construction and Building Materials*, *101*, 702–709. https://doi.org/10.1016/j.conbuildmat.2015.10.047

Bencardino, F., Rizzuti, L., Spadea, G., & Swamy, R. N. (2008). Stress-strain behavior of steel fiber-reinforced concrete in compression. *Journal of Materials in Civil Engineering*, *20*(3), 255–263. https://doi.org/10.1061/(ASCE)0899-1561(2008)20:3(255)

Bentur, A., & Mindess, S. (1990). *Fiber reinforced cementitious composites*. Elsevier Applied Science.

Bhutta, M. A. R., Ariffin, N. F., Hussin, M. W., & Lim, N. H. A. S. (2013). Sulfate and sulfuric acid resistance of geopolymer mortars using waste blended ash. *Jurnal Teknologi*, *61*(3), 1–5. https://doi.org/10.11113/jt.v61.1762

Bhutta, A., Borges, P. H., Zanotti, C., Farooq, M., & Banthia, N. (2017). Flexural behavior of geopolymer composites reinforced with steel and polypropylene macro fibers. *Cement and Concrete Composites*, *80*, 31–40. https://doi.org/10.1016/j.cemconcomp.2016.11.014

British Standard Institution BS EN 12390-3. (2009). *Testing hardened concrete, compressive strength of test specimens*.

Chabrelie, A. (2010). *Mechanisms of degradation of concrete by external sulfate ions under laboratory and field conditions* [PhD thesis]. École Polytechnique Fédérale De Lausanne.

Colangelo, F., & Cioffi, R. (2017). Mechanical properties and durability of mortar containing fine fraction of demolition wastes produced by selective demolition in South Italy. *Composites Part B: Engineering*, *115*, 43–50. https://doi.org/10.1016/j.compositesb.2016.10.045

Davidovits, J. (1991). Geopolymers: inorganic polymeric new materials. *Journal of Thermal Analysis*, *37*(8), 1633–1656. https://doi.org/10.1007/BF01912193

Davidovits, J. (1994). *Properties of geopolymer cements* [Paper presentation]. First International Conference on Alkaline Cements and Concretes, (October). (Vol. 1, pp. 131–149). Kiev, Ukraine: Kiev State Technical University.

Duxson, P., Lukey, G. C., & van Deventer, J. S. (2007). Physical evolution of Na-geopolymer derived from metakaolin up to 1000 C. *Journal of Materials Science*, *42*(9), 3044–3054. https://doi.org/10.1007/s10853-006-0535-4

E.C. (European Commission), Directorate-General Environment, Directorate Industry and Environment. (2000). ENV.E.3-Waste Management, Management of Construction and Demolition Waste Working Document No. I.

Ebrahimi, A., Saffari, M., Milani, D., Montoya, A., Valix, M., & Abbas, A. (2017). Sustainable transformation of fly ash industrial waste into a construction cement blend via CO_2 carbonation. *Journal of Cleaner Production*, *156*, 660–669. https://doi.org/10.1016/j.jclepro.2017.04.037

European Standard EN 1338. (2003). Concrete Paving Blocks - requirements and test methods.

Faisal, F. W., & Ashour, S. A. (1992). Mechanical properties of high-strength fiber reinforced concrete. *ACI Material Journal*, *89*(5), 449–455.

Ganesan, N., Abraham, R., & Raj, S. D. (2015). Durability characteristics of steel fibre reinforced geopolymer concrete. *Construction and Building Materials*, *93*, 471–476. https://doi.org/10.1016/j.conbuildmat.2015.06.014

Gao, J., Sun, W., & Morino, K. (1997). Mechanical properties of steel fiber-reinforced, high-strength, lightweight concrete. *Cement and Concrete Composites*, *19*(4), 307–313. https://doi.org/10.1016/S0958-9465(97)00023-1

García-Lodeiro, I., Palomo, A., Fernández-Jiménez, A., & Macphee, D. E. (2011). Compatibility studies between NASH and CASH gels. Study in the ternary diagram Na2O–CaO–Al2O3–SiO2–H2O. *Cement and Concrete Research*, *41*(9), 923–931. https://doi.org/10.1016/j.cemconres.2011.05.006

Gök, A., Omastova, M., & Prokeš, J. (2007). Synthesis and characterization of red mud/polyaniline composites: electrical properties and thermal stability. *European Polymer Journal*, *43*(6), 2471–2480. https://doi.org/10.1016/j.eurpolymj.2007.03.005

Gomes, R. F., Dias, D. P., & de Andrade Silva, F. (2020). Determination of the fracture parameters of steel fiber-reinforced geopolymer concrete. *Theoretical and Applied Fracture Mechanics*, *107*, 102568. https://doi.org/10.1016/j.tafmec.2020.102568

Guo, X., & Pan, X. (2018). Mechanical properties and mechanisms of fiber reinforced fly ash–steel slag based geopolymer mortar. *Construction and Building Materials*, *179*, 633–641. https://doi.org/10.1016/j.conbuildmat.2018.05.198

Hannant, D. J. (1978). *Fibre cements and fibre concretes*. John Wiley & Sons.

Hardjito, D., Wallah, S. E., Sumajouw, D. M., & Rangan, B. V. (2004). On the development of fly ash-based geopolymer concrete. *Materials Journal*, *101*(6), 467–472.

Hwang, J. P., Shim, H. B., Lim, S., & Ann, K. Y. (2013). Enhancing the durability properties of concrete containing recycled aggregate by the use of pozzolanic materials. *KSCE Journal of Civil Engineering*, *17*(1), 155–163. https://doi.org/10.1007/s12205-013-1245-5

Ismail, I., Bernal, S. A., Provis, J. L., San Nicolas, R., Hamdan, S., & van Deventer, J. S. (2014). Modification of phase evolution in alkali-activated blast furnace slag by the incorporation of fly ash. *Cement and Concrete Composites*, *45*, 125–135. https://doi.org/10.1016/j.cemconcomp.2013.09.006

Junru, R., Huiguo, C., Ruixi, D., & Tao, S. (2019). *Behavior of combined fly ash/GBFS-based geopolymer concrete after exposed to elevated temperature* [Paper presentation]. In IOP Conference Series: Earth and Environmental Science, (May). (Vol. *267*, No. 3, p. 032056). IOP Publishing. https://doi.org/10.1088/1755-1315/267/3/032056

Khoury, G. A. (2000). Effect of fire on concrete and concrete structures. *Progress in Structural Engineering and Materials*, *2*(4), 429–447. https://doi.org/10.1002/pse.51

Kumar, S., Kumar, R., & Mehrotra, S. P. (2010). Influence of granulated blast furnace slag on the reaction, structure and properties of fly ash based geopolymer. *Journal of Materials Science*, *45*(3), 607–615. https://doi.org/10.1007/s10853-009-3934-5

Kuranlı, Ö. F., Uysal, M., Abbas, M. T., Çoşgun, T., Niş, A., Aygörmez, Y., Canpolat, O., & Al-Mashhadani, M. M. (2023). Mechanical and durability properties of steel, polypropylene, and polyamide fiber reinforced slag-based alkali-activated concrete. *European Journal of Environmental and Civil Engineering*, *27*(1), 114–139. https://doi.org/10.1080/19648189.2022.2031302

Kurda, R., Silvestre, J. D., & de Brito, J. (2018). Life cycle assessment of concrete made with high volume of recycled concrete aggregates and fly ash. *Resources, Conservation and Recycling*, *139*, 407–417. https://doi.org/10.1016/j.resconrec.2018.07.004

Kurtoglu, A. E., Alzeebaree, R., Aljumaili, O., Nis, A., Gulsan, M. E., Humur, G., & Cevik, A. (2018). Mechanical and durability properties of fly ash and slag based geopolymer concrete. *Advances in Concrete Construction*, *6*(4), 345. https://doi.org/10.12989/acc.2018.6.4.345

Laneyrie, C., Beaucour, A. L., Green, M. F., Hebert, R. L., Ledesert, B., & Noumowe, A. (2016). Influence of recycled coarse aggregates on normal and high performance concrete subjected to elevated temperatures. *Construction and Building Materials*, *111*, 368–378. https://doi.org/10.1016/j.conbuildmat.2016.02.056

Lee, N. K., Abate, S. Y., & Kim, H. K. (2018). Use of recycled aggregates as internal curing agent for alkali-activated slag system. *Construction and Building Materials*, *159*, 286–296. https://doi.org/10.1016/j.conbuildmat.2017.10.110

Liu, Z., Cai, C. S., Peng, H., & Fan, F. (2016). Experimental study of the geopolymeric recycled aggregate concrete. *Journal of Materials in Civil Engineering*, *28*(9), 04016077. https://doi.org/10.1061/(ASCE)MT.1943-5533.0001584

Malhotra, V. M. (2002). High-performance high-volume fly ash concrete. *Concrete International*, *24*(7), 30–34.

Marie, I., & Quiasrawi, H. (2012). Closed-loop recycling of recycled concrete aggregates. *Journal of Cleaner Production*, *37*, 243–248. https://doi.org/10.1016/j.jclepro.2012.07.020

Marinković, S., Radonjanin, V., Malešev, M., & Ignjatović, I. (2010). Comparative environmental assessment of natural and recycled aggregate concrete. *Waste Management (New York, NY)*, *30*(11), 2255–2264. https://doi.org/10.1016/j.wasman.2010.04.012

Mesgari, S., Akbarnezhad, A., & Xiao, J. Z. (2020). Recycled geopolymer aggregates as coarse aggregates for Portland cement concrete and geopolymer concrete: Effects on mechanical properties. *Construction and Building Materials*, *236*, 117571. https://doi.org/10.1016/j.conbuildmat.2019.117571

Mustafa Al Bakri, A. M., Kamarudin, H., Bnhussain, M., Rafiza, A. R., & Zarina, Y. (2012). Effect of Na2SiO3/NaOH Ratios and NaOH Molarities on compressive strength of fly-ash-based geopolymer. *ACI Materials Journal*, *109*(5), 503–508.

Naaman, A. E. (1985). Fiber reinforcement for concrete. *Concrete Int.: Des. Construct*, *7*(3), 21–25.

Neville, A. M. (1996). *Properties of concrete: Fourth and final edition* (4th ed.). Wiley.

Niş, A., Eren, N. A., & Çevik, A. (2023). Effects of recycled tyre rubber and steel fibre on the impact resistance of slag-based self-compacting alkali-activated concrete. *European Journal of Environmental and Civil Engineering*, *27*(1), 519–537. https://doi.org/10.1080/19648189.2022.2052967

Novák, J., & Kohoutková, A. (2017). *Fibre reinforced concrete exposed to elevated temperature* [Paper presentation]. In IOP Conference Series: Materials Science and Engineering, (September). (Vol. *246*, No. 1, p. 012045). IOP Publishing. https://doi.org/10.1088/1757-899X/246/1/012045

Nuaklong, P., Sata, V., & Chindaprasirt, P. (2016). Influence of recycled aggregate on fly ash geopolymer concrete properties. *Journal of Cleaner Production*, *112*, 2300–2307. https://doi.org/10.1016/j.jclepro.2015.10.109

Padmini, A. K., Ramamurthy, K., & Mathews, M. S. (2009). Influence of parent concrete on the properties of recycled aggregate concrete. *Construction and Building Materials*, *23*(2), 829–836. https://doi.org/10.1016/j.conbuildmat.2008.03.006
Ping, W., & Yidong, X. (2011). Life cycle assessment of recycled aggregate concrete containing fly ash. In *2011 Second International Conference on Mechanic Automation and Control Engineering* (pp. 2287–2290). IEEE. https://doi.org/10.1109/MACE.2011.5987436
Plank, J., & Winter, C. (2008). Competitive adsorption between superplasticizer and retarder molecules on mineral binder surface. *Cement and Concrete Research*, *38*(5), 599–605. https://doi.org/10.1016/j.cemconres.2007.12.003
Potrzebowski, J. (1983). The splitting test applied to steel fibre reinforced concrete. *International Journal of Cement Composites and Lightweight Concrete*, *5*(1), 49–53. https://doi.org/10.1016/0262-5075(83)90048-9
Prabua, B., Kumuthab, R., & Vijaib, K. (2017). Effect of fibers on the mechanical properties of fly ash and GGBS based geopolymer concrete under different curing conditions. *Indian Journal of Engineering & Materials Sciences*, *24*, 5–12.
Provis, J. L., Palomo, A., & Shi, C. (2015). Advances in understanding alkali-activated materials. *Cement and Concrete Research*, *78*, 110–125. https://doi.org/10.1016/j.cemconres.2015.04.013
Rakhimova, N. R., Rakhimov, R. Z., Morozov, V. P., Gaifullin, A. R., Potapova, L. I., Gubaidullina, A. M., & Osin, Y. N. (2018). Marl-based geopolymers incorporated with limestone: A feasibility study. *Journal of Non-Crystalline Solids*, *492*, 1–10. https://doi.org/10.1016/j.jnoncrysol.2018.04.015
Rangan, B. V. (2008). Mix design and production of flyash based geopolymer concrete. *The Indian Concrete Journal*, *82*(5), 7–15. https://doi.org/10.1007/978-81-322-2187-6_123
Ranjbar, N., Mehrali, M., Mehrali, M., Alengaram, U. J., & Jumaat, M. Z. (2016). High tensile strength fly ash based geopolymer composite using copper coated micro steel fiber. *Construction and Building Materials*, *112*, 629–638. https://doi.org/10.1016/j.conbuildmat.2016.02.228
Rees, C. A., Provis, J. L., Lukey, G. C., & van Deventer, J. S. (2007). Attenuated total reflectance fourier transform infrared analysis of fly ash geopolymer gel aging. *Langmuir: The ACS Journal of Surfaces and Colloids*, *23*(15), 8170–8179. https://doi.org/10.1021/la700713g
Sai, A. (2018). An experimental study on strength properties of concrete using recycled aggregate as replacement in coarse aggregate. *International Journal for Research in Applied Science and Engineering Technology*, *6*(2), 665–676. https://doi.org/10.22214/ijraset.2018.2124
Sanni, S. H., & Khadiranaikar, R. B. (2012). Performance of geopolymer concrete under severe environmental conditions. *International Journal of Civil and Structural Engineering*, *3*(2), 396–407.
Sarhat, S. R., & Sherwood, E. G. (2013). Residual mechanical response of recycled aggregate concrete after exposure to elevated temperatures. *Journal of Materials in Civil Engineering*, *25*(11), 1721–1730. https://doi.org/10.1061/(ASCE)MT.1943-5533.0000719
Sata, V., Wongsa, A., & Chindaprasirt, P. (2013). Properties of pervious geopolymer concrete using recycled aggregates. *Construction and Building Materials*, *42*, 33–39. https://doi.org/10.1016/j.conbuildmat.2012.12.046
Schneider, M., Romer, M., Tschudin, M., & Bolio, H. (2011). Sustainable cement production—present and future. *Cement and Concrete Research*, *41*(7), 642–650. https://doi.org/10.1016/j.cemconres.2011.03.019
Sukontasukkul, P., Pongsopha, P., Chindaprasirt, P., & Songpiriyakij, S. (2018). Flexural performance and toughness of hybrid steel and polypropylene fibre reinforced geopolymer. *Construction and Building Materials*, *161*, 37–44. https://doi.org/10.1016/j.conbuildmat.2017.11.122
Sun, J. Y., et al. (2015). *Policy study on recycling and reuse of construction and demolish waste [R]* (p. 5). the P.R.C. Building Industry Press.
Taylor, M., Tam, C., & Gielen, D. (2006). Energy efficiency and CO_2 emissions from the global cement industry. *Korea*, *50*(2.2), 61–67.
Thomas, J., Thaickavil, N. N., & Wilson, P. M. (2018). Strength and durability of concrete containing recycled concrete aggregates. *Journal of Building Engineering*, *19*, 349–365. https://doi.org/10.1016/j.jobe.2018.05.007
Topal, Ö., Karakoç, M. B., & Özcan, A. (2022). Effects of elevated temperatures on the properties of ground granulated blast furnace slag (GGBFS) based geopolymer concretes containing recycled concrete aggregate. *European Journal of Environmental and Civil Engineering*, *26*(10), 4847–4862. https://doi.org/10.1080/19648189.2021.1871658

Xie, J. H., Guo, Y. C., Liu, L. S., & Xie, Z. H. (2015). Compressive and flexural behaviours of a new steel-fibre-reinforced recycled aggregate concrete with crumb rubber. *Construction and Building Materials*, *79*, 263–272. https://doi.org/10.1016/j.conbuildmat.2015.01.036

Xie, J., Zhao, J., Wang, J., Wang, C., Huang, P., & Fang, C. (2019). Sulfate resistance of recycled aggregate concrete with GGBS and fly ash-based geopolymer. *Materials*, *12*(8), 1247. https://doi.org/10.3390/ma12081247

Yan, X., Li, H., & Wong, Y. L. (2007). Effect of aggregate on high-strength concrete in fire. *Magazine of Concrete Research*, *59*(5), 323–328. https://doi.org/10.1680/macr.2007.59.5.323

Ye, H., & Radlińska, A. (2016). Fly ash-slag interaction during alkaline activation: Influence of activators on phase assemblage and microstructure formation. *Construction and Building Materials*, *122*, 594–606. https://doi.org/10.1016/j.conbuildmat.2016.06.099

Zaid, O., Martínez-García, R., Abadel, A. A., Fraile-Fernández, F. J., Alshaikh, I. M., & Palencia-Coto, C. (2022). To determine the performance of metakaolin-based fiber-reinforced geopolymer concrete with recycled aggregates. *Archives of Civil and Mechanical Engineering*, *22*(3), 1–14. https://doi.org/10.1007/s43452-022-00436-2